

# **Upscaling of in-situ measurements using spatially distributed model simulations for validation of satellite soil moisture products**

MOHAMMAD SHAHMOHAMMADI MEHRJARDI

UNIVERSITY OF TWENTE, Enschede, the Netherlands

February 2016

Thesis submitted to the Faculty of Geo-Information Science and Earth Observation of the University of Twente in partial fulfillment of the requirements for the degree of Master of Science in Geo-information Science and Earth Observation. Specialization: Water Resources and Environmental Management (WREM)

**SUPERVISORS:**

Dr. Ir. Rogier van der Velde

Dr. Ir. Mhd. Suhyb Salama

**THESIS ASSESSMENT BOARD:**

Prof. W. Verhoef (chair)

Dr. D.M.D. Hendriks (External Examiner)



#### DISCLAIMER

This document describes work undertaken as part of a programme of study at the Faculty of Geo-Information Science and Earth Observation of the University of Twente. All views and opinions expressed therein remain the sole responsibility of the author, and do not necessarily represent those of the Faculty

# ABSTRACT

*In-situ* soil moisture measurements collected by 20 monitoring stations located in Twente region are employed to assess the reliability of three surface soil moisture spatially distributed products. One simulated soil moisture from Land Hydrological Model (LHM) and two satellite-based coarse resolution soil moisture products, namely SMOS L3 (Soil Moisture Ocean Salinity Level 3) and SMAP L2 P (Soil Moisture Active Passive Level 2 Passive). First the reliability of the each spatially distributed product is evaluated by measurement obtained from the individual station. Then the LHM product is employed to derive and develop up-scaling functions for transferring point measurements to domain scale. Finally, *in-situ* up-scaled soil moisture measurements are used to evaluate the satellite product. Time series analysis demonstrates that the LHM product at measurement location follows temporal dynamic of *in-situ* measurements in the summer period and two remotely sensed products capture the temporal dynamic of surface soil moisture. However, for satellite-based soil moisture overestimation in wet condition and underestimation for dry situation are observed. Dry biases and different respond to precipitation are observed for three products. Correlation values between *in-situ* and satellite observations are found very satisfactory with the value of 0.82 for SMAP and average value of 0.60 for SMOS and 0.32 for LHM. The SMAP product fulfils the accuracy requirement by the satellite mission, root mean squared differences (RMSD) of  $0.06 \text{ m}^3.\text{m}^{-3}$  and centred root mean squared of  $0.04 \text{ m}^3.\text{m}^{-3}$  are found for SMAP product, while for the SMOS product average RMSD of  $0.10\text{m}^3.\text{m}^{-3}$  are observed.

**Keywords:** Remotely sensed surface soil moisture, SMAP, SMOS, *in-situ* soil moisture, Land Hydrological Model

# ACKNOWLEDGEMENTS

I would like to express my heartfelt thanks to my family for supporting me through all steps of my life.

I would like to express my sincere thanks to my supervisors Dr. Rogier Van der Velde and Dr. Suhyb Salama for their helps and supports. This thesis would not successfully complete without your guidance.

I would like to acknowledge Joachim Hunink and Dimmie Hendriks (Deltares) for giving access to the LHM soil moisture datasets.

# TABLE OF CONTENTS

---

Abstract.....	ii
Acknowledgements.....	iii
List of figures.....	v
List of tables.....	vi
1. Introduction.....	1
1.1. Scientific Background.....	1
1.2. Research objectives.....	3
1.3. Research questions.....	4
1.4. Thesis outline.....	4
2. Study area and in-situ data set.....	5
2.1. Twente Region.....	5
2.2. In-situ Monitoring Network.....	5
2.3. Field Experiment.....	5
3. Spatial data sets.....	7
3.1. Remotely sensed surface soil moisture.....	7
3.1.1. SMOS global daily soil moisture product level 3(L3 SM).....	7
3.1.2. SMAP radiometer soil moisture product level 2 (L2_SM_P).....	8
3.2. Land Hydrological Model (LHM) soil moisture simulation.....	10
4. Method.....	11
4.1. Upscaling strategies.....	11
4.1.1. Simple averaging.....	11
4.1.2. Enhanced upscaling using distributed land surface modelling.....	11
4.2. Assessment metrics.....	12
5. Model-based up-scaling.....	14
5.1. Time series analysis.....	14
5.2. Taylor diagram.....	18
5.3. Soil moisture aggregated across the study domain.....	20
5.4. Upscaling functions.....	22
6. Assessment of satellite-based products.....	24
6.1. Comparison of individual stations with SMOS L3 SM.....	24
6.2. Comparison of individual stations with SMAP L2 SM P.....	27
6.3. Comparison of upscaled in situ soil moisture with satellite observations.....	30
7. Final Remarks.....	35
7.1. Conclusion.....	35
7.2. Recommendation.....	36
List of references.....	37
Appendix.....	40

## LIST OF FIGURES

---

Figure 1 shows Land cover maps of Twente region and location of soil moisture stations with black circle symbol .....	6
Figure 2: The schematic overview of processing L3 SM (Kerr et al., 2014).....	8
Figure 3, simplified schematic processing flow of SMAP L2-SM-P (Entekhabi et al., 2014).....	9
Figure 4, temporal evaluation of individual <i>in-situ</i> measurements and simulated surface soil moisture in measurement locations along with daily rainfall in 2012 are presented.....	15
Figure 5, presents Taylor diagrams demonstrating results of comparison among individual <i>in-situ</i> measurements, annual (left) and summer (right) simulated product at measurements location for 2012 (top), 2013 ( middle) and 2014 (bottom). Only stations with positive correlation are presented. ....	19
Figure 6 time series of the averaged simulated soil moisture at measurement locations along with spatially averaged over the whole domain and daily precipitation for 2012 (Top), 2013 (Middle) and 2014 (Bottom). ....	21
Figure 7 scatter plots of averaged simulated soil moisture at measurement locations (LHM station) and the bias corrected mean <i>in-situ</i> soil moisture measurement for the summer period of years 2012, 2013 and 2014.....	22
Figure 8 scatter plots of $\theta_{pixel}$ (stations) and $\theta_{Domain}$ (model domain) and for years 2012, 2013, 2014 and 2015. ....	23
Figure 9 presents correlation between SMOS L3 SM and in situ data for individual stations in 2015. ....	26
Figure 10, presents scatter plots between SMAP L2 SM P and individual stations from a period of first of April to November 31. ....	28
Figure 11 presents statistical scores of comparison between SMOS, SMAP and particular in situ measurements in 2015. ....	29
Figure 12 soil moisture evaluation of in-situ measurements (average of station and upscaled) LHM product and SMOS and SMAP observation along with daily rainfall in Twente region. ....	32
Figure 13 demonstrates results of comparison between mean in-situ measurement $\theta_{point}$ and SMOS observation for years 2012, 2013, 2014 and 2015 .....	33
Figure 14 demonstrates results of comparison between mean in-situ measurement $\theta_{Domainpoint}$ and SMOS observation for years 2012, 2013, 2014 and 2015. ....	33
Figure 15 illustrates scatter plots between mean in-situ measurement( $\theta_{point}$ ), upscaled in-situ measurement ( $\theta_{Domainpoint}$ ) and SMAP observation.....	34
Figure 16, temporal evaluation of individual in situ measurements and simulated surface soil moisture in measurement locations along with rainfall in 2013 .....	42
Figure 17, temporal evaluation of individual in situ measurements and simulated surface soil moisture in measurement locations along with rainfall in 2014 .....	46

## LIST OF TABLES

---

Table 1, Pearson correlation(R), root mean squared differences (RMSD) and bias between individual station measurements and original LHM product for 2012, 2013 and 2014 are presented.....	16
Table 2 presents statistical results of comparison between <i>in-situ</i> measurements and LHM product in summer period of years 2012, 2013 and 2014.....	17
Table 3 gives statistical result of comparison between simulated soil moisture at measurements location ( $\theta_{pixel}$ ) and averaged simulated product over entire domain ( $\theta_{Domain}$ ).....	20
Table 4 presents statistical result of comparison between simulated soil moisture at measurements location ( $\theta_{pixel}$ ) and bias corrected mean <i>in-situ</i> soil moisture measurement ( $\theta_{pointcor}$ ).....	21
Table 5 presents slopes and intercepts of up-scaling functions along with coefficient determination between $\theta_{pixel}$ and $\theta_{Domain}$ datasets for years 2012, 2013 and 2014.....	23
Table 6 Pearson correlation (R), root mean squared differences (RMSD) and bias between individual station measurements and SMOSL3 for 2010, 2011 and 2012.....	24
Table 7 Pearson correlation (R), root mean squared differences (RMSD) and bias between individual station measurements and SMOSL3 for 2013, 2014 and 2015.....	25
Table 8 statistical results of comparison between SMAP L2 SM P and individual stations form April till November 2015.....	27
Table 9 presents statistics of comparison among <i>in-situ</i> measurements (average of station and upscaled), SMOS and SMAP observations for years 2012, 2013, 2014 and 2015.....	31

# 1. INTRODUCTION

## 1.1. Scientific Background

Soil moisture comprises just 0.15% of global liquid fresh water but, it is a key variable in meteorological, hydrological, agricultural and climatological studies (Western et al., 2002; Du, 2012). From a meteorological aspect, soil moisture governs the partitioning of incoming radiation at land surface. Moreover, latent and sensible heat fluxes also plays a vital role in global climate and weather system (Xia et al., 2014; Petropoulos et al., 2015). In hydrology, soil moisture is a significant component that controls rainfall partitioning to surface runoff and infiltration, which has a direct effect on groundwater recharge and streamflow (Tuttle & Salvucci, 2014). From an agricultural point of view, soil moisture controls sustainable agriculture and crop growth. Regarding the pieces of evidence, it is arguable that soil moisture, in fact, is a core of the system that determines hydrological interaction among atmospheric forcing, soil and vegetation. Hence, it is essential to obtain accurate and detailed soil water content information in both space and time to facilitate efficient water management and sustainable agriculture (Heathman et al., 2012; Brocca et al., 2011).

There are numerous methods to estimate soil moisture, which can be distinguished into in-situ measurements, earth observation data and process modelling approach. However, integration of two or three techniques allows overcoming drawbacks of every individual method (Brocca et al., 2011). Ground measurements provides the most accurate and reliable ( $\sim 0.04 \text{ m}^3 \text{ m}^{-3}$ ) soil moisture estimation with high temporal resolution and the possibility of measurements at various depths on the ground, although it is limited in terms of spatial extent. Therefore, they are not entirely sufficient to obtain spatial and temporal variability of soil moisture on a large scale (Brocca et al., 2011; Brocca et al., 2010; Petropoulos et al., 2015; Zeng, Li, Chen, & Bi, 2014). On the other hand, satellite microwave remote sensing with a daily (or even higher) revisit time are not only the most practical method for global estimation of soil moisture, but also could be applied for calibration and validation of hydrological models (Brocca et al., 2011; Houser, De lannoy, & Walker, 2010; Su et al., 2014).

Microwave remote sensing provides quantitative soil moisture information by detecting changes within electrical permittivity of the soil. Particularly in low frequency (1-5 GHz) while the atmosphere is relatively transparent (Petropoulos et al., 2015; Qiu et al., 2013). Operational sensors that have been used for soil moisture estimation include WindSat (a polarimetric microwave radiometer, HH-VV polarization, 6.8–37 GHz, onboard the Coriolis satellite launched in 2003), AMSR-E (Advance Microwave Scanning Radiometer for the Earth Observing system, HH-VV polarization, 6.9-89 GHz onboard the Aqua satellite launched 2002), ASCAT (Advance Scatterometer, VV polarization, 5.225 GHz on-board the meteorological satellite Metop-A launched in 2006) (Brocca et al., 2011).

All mentioned instruments have been operating at frequency above 5 GHz. Numerous studies have shown that remotely sensed soil moisture estimation in microwave L-band (1.4 GHz) is considered the most promising technique not only because of lower influence of vegetation but also because L-band is more sensitive to the water content. Moreover, it is more sensitive to soil moisture in deeper soil layer, approximately 0 – 10 cm of surface layer (Gherboudj et al., 2012; Rötzer et al., 2014; Entekhabi et al., 2014). Therefore, in November 2009, the Soil Moisture and Ocean Salinity (SMOS) satellite was launched by the European Space Agency (ESA). It is the first satellite dedicated to measure soil moisture and ocean salinity on global scale consisting of a space borne L-band (1.4 GHz) (Kerr et al., 2001). SMOS is an all-weather system with aim of global soil moisture mapping less than 3 days at spatial resolution of less than 50 km (Bitar et al., 2012; Kerr et al., 2001).

The specified sensors are characterized as a coarse spatial resolution (~25-50 km), which are more suitable for hydro-climate studies. While, the availability of moderate spatial resolution (10 km) soil moisture data would improve understanding and forecasting of regional weather system around the world, also it enhances agricultural-related applications and large watershed management activities (Brocca et al., 2010; Das, Entekhabi, & Njoku, 2011; Panciera et al., 2014).

The National Aeronautics and Space Administration (NASA) launched soil moisture active and passive (SMAP) mission in January 2015 to respond to hydrometeorological application needs. The SMAP is carrying the first integrated L-band radiometer (1.41 GHz; H, V) and L-band radar (SAR) system (1.26 GHz; HH, VV, HV polarization) specifically dedicated to soil moisture monitoring (Das et al., 2011; Panciera et al., 2014). It provides three different types of global soil moisture maps high (3km), moderate (9 km) and coarse (36 km) resolutions within three days at equator and two days at latitude higher than 45°.

Since remotely sensed soil moisture observations are hampered by numerous factors such as atmospheric conditions, soil surface-roughness and vegetation, assessment of the accuracy and reliability of the data science products before using them is crucial. Normally, verification of remotely sensed products contains two objectives, the first aim is that the algorithm developers could get feedback from validation results and employ it for further the algorithm improvement, and the second is to assess the potential users to be aware of products status (Zeng et al., 2015).

Various methodologies can be implemented for validation purposes, which include ground-based soil moisture networks, short-term airborne data acquisitions with intense ground sampling and simulated products, which either can be result of multi-model soil moisture or via assimilation systems that land surface models and related soil moisture observation have been combined (Jackson et al., 2012).

Validation of coarse spatial resolution of satellite based soil moisture products with in situ measurements has always been challenging not only because of the disparity in spatial scales between products but also because of requirements of continuous long-term observation to provide sufficient range of soil moisture and seasonal patterns. Additionally, a robust validation must include various soil types, climate conditions and vegetation covers (T. J. Jackson et al., 2012; N. Sánchez et al., 2012).

On the other hand, land surface models can be used as an alternative source of surface soil moisture for validation of remotely sensed products. In these models, spatially distributed data such as soil type, land use, topography, meteorological forcing are synthesized and reliable soil moisture production is predicted over a large spatial area (Crow et al., 2012; Crow, Ryu, & Famiglietti, 2005). Since the input data are distributed, the simulated soil moisture products are not influenced by deficit of sampling density compared to ground-based measurements. However, systematic differences between simulated products and in situ measurements may exist, which can be suppressed by various developed techniques such as linear regression correction, rescaling, and cumulative density function, CDF, matching (Brocca et al., 2011).

Another possible approach for validation of satellite soil moisture retrieval is based on combination of in situ measurements with spatially distributed models which consist of data assimilation strategy and model calibration technique. A basic assumption in this method is that model output contains relative relationship between average of soil moisture at given measurement location and spatially averaged soil moisture within some large regional area (Crow et al., 2005). If this relation exists then in situ measurements and simulated product can be integrated to enhance retrieved foot-print soil moisture average.

This research presents the accuracy assessment of surface soil moisture estimates from SMOS and SMAP sensors using "ground truth" soil moisture data developed from a combination of in-situ measurements and model simulations in Twente region. Along with satellite-based datasets LHM spatially distributed soil moisture simulated product is evaluated and employed to drive up-scaling function for transferring in-situ point measurements to satellite foot prints.

## **1.2. Research objectives**

The main objective of the research is to validate remotely sensed soil moisture products using soil moisture data developed from a combination of in-situ measurements and model simulations.

The specific objectives can be formulated as follows:

- To evaluate the reliability of the spatially distributed soil moisture simulated by LHM using *in-situ* measurements collected in the Twente region;
- To develop an up-scaling function to transfer the point-scale *in-situ* measurements to domain-scale using the LHM spatially distributed soil moisture products;
- To validate satellite products (e.g. SMOS L3, SMAP L2) using *in-situ* soil moisture (individual and averaged) measured at the individual monitoring stations;
- To validate satellite products (e.g. SMOS L3, SMAP L2) using up-scaling *in-situ* soil moisture measurements.

### 1.3. Research questions

- How reliable is the performance of LHM simulation of soil moisture regarding in-situ measurements in Twente region?
- What is the difference between the model upscaled soil moisture and mean soil moisture derived from the individual stations?
- Do remotely sensed soil moisture products (SMOS L3, SMAP\_L2\_P) achieve their scientific accuracy requirement ( $0.04\text{m}^3\cdot\text{m}^{-3}$ ) towards upscaled simulated soil moisture data in Twente region?
- How does the use of the model-based upscaled soil moisture affect the validation results over the mean soil moisture derived from individual stations?

### 1.4. Thesis outline

Chapter 1 (the present one) presents an introduction to the background, research objectives, research questions and the outline of the study. Brief description of the study area, soil moisture monitoring network and field experiment are described in chapter 2. Chapter 3 gives detailed remotely sensed and simulated soil moisture products. Chapter 4 provides methodologies and metrics that are used for assessment of spatially distributed soil moisture products. The results of LHM product evaluation and the process of deriving and developing up-scaling function are explained in chapter 5. Chapter 6 provides the assessment results of satellite-based products. Chapter 7 outlines conclusion and recommendations of the study.

## 2. STUDY AREA AND IN-SITU DATA SET

### 2.1. Twente Region

Twente is a region located in the eastern part of Overijssel province of the Netherlands with geographical coordinates of 52°05' - 52°27' N latitude and 6° 05' -7° 00' E longitude. Topography of Twente is almost flat with elevation between 3 m and 50 m above sea level. Twente is bisected by a range of hills distributed from the west to the east, with the highest point near Oldenzaal city in the east of the region. Land cover in the region is heterogeneous and consists of urban, agricultural, forested area and dominated grassland used for livestock grazing.

The Twente region lies in oceanic climate with mild winter and summer according to Köppen climate classification system (Group C). Monthly average air temperature range is between 3°C and 17°C in January and July respectively. Precipitation is almost evenly distributed over a year summing up to an annual average of about 765 mm. Sandy soils, loam soils, man-made sandy thick earth soils and peat soils covered by layer of peat or sand are the four main soil types of Twente region. Sand and loamy sands are, however, most common soil types in the near surface (Dente, Su, & Wen, 2012; Dente et al., 2011)

### 2.2. In-situ Monitoring Network

The Faculty of Geo-Information Science and Earth Observation (ITC) of the University of Twente provides a soil moisture and soil temperature monitoring network consisting of twenty stations that cover an area of approximately 50 km × 40 km. The site is equipped with EC-TM ECH2O probes (Decagon Devices, Inc., USA) for the measurement of soil moisture and soil temperature at a depth of 5 cm as well as deeper layers every 15 min since July 2009. The stations are distributed across the area to represent different land cover and soil types. Sixteen stations were installed in grassland and meadow, which normally are used for grazing; one of them was set up in forested area and three stations in corn field.

### 2.3. Field Experiment

In-situ soil moisture measurements are the most reliable data that can be employed to evaluate modelled and remotely sensed soil moisture observation. Soil moisture varies spatially through complicated interaction among pedologic, topographic, vegetative and meteorological factors (Crow et al., 2012). Twente region is topographically and meteorologically fairly homogeneous. Consequently, soil heterogeneity and vegetation cover have been selected as variables for the design of the sampling strategy.

The soil analysis for a layer near the surface, i.e. from 0 to 40 cm depth demonstrated 7 stations (ITCSM\_08, ITCSM\_10, ITCSM\_13, ITCSM\_15, ITCSM\_17, ITCSM\_19 and ITCSM\_20) are located in fine sand; 3 sites (ITCSM\_03, ITCSM\_14, ITCSM\_18) are installed in loamy fine sand; 4 sites (ITCSM\_02, ITCSM\_05, ITCSM\_09, ITCSM\_11) are built up in man-made sandy thick earth soil; 3 sites (ITCSM\_01, ITCSM\_07, ITCSM\_12) are installed sandy clay loam on subsoil of fine sand; and station ITCSM\_04 is set up in loam (Dente et al., 2011). As such, stations ITCSM\_03, ITCSM\_04, ITCSM\_5,

ITCSM\_7, ITCSM\_8 and ITCSM\_9 have been selected as being representative for the soils type available in the study area.

In order to check how representative the stations are for the area, two or three different fields near each station with various vegetation covers were selected for sampling. In every field, 15 and 30 independent soil moisture content were measured with Theta Probe instruments. The instrument estimate volumetric soil moisture with differences between output wave and return wave frequency. Frequency domain Reflectometry (FDR) probes are considered as accurate instrument but must be calibrated. Therefore, three gravimetric samples were taken near to probe measurements to be used for calibration and validation of instrument measurements. Normally, Points were selected in the middle of fields for avoiding edge effects, where soil and vegetation conditions might not be representative for the field. In addition, soil moisture was measured during a period of September 11<sup>th</sup> to November 3<sup>rd</sup> to assess stations for all possible dynamic range of soil moisture content.

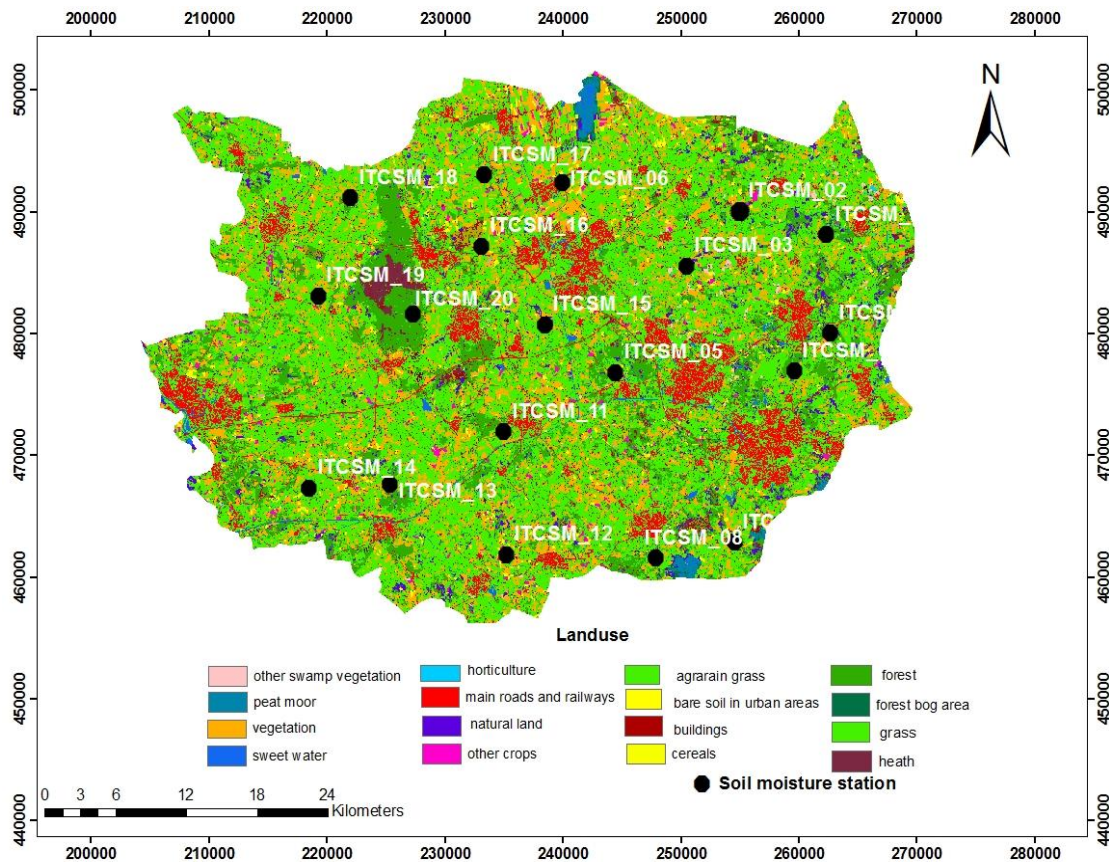


Figure 1 shows Land cover maps of Twente region and location of soil moisture stations with black circle symbol

## 3.SPATIAL DATA SETS

### 3.1. Remotely sensed surface soil moisture

#### 3.1.1. SMOS global daily soil moisture product level 3(L3 SM)

The SMOS mission is a joint program led by European Space Agency (ESA) in contribution with Center National d'Etudes spatiales (CNES) in France and Centro para el Desarrollo Tecnológico Industrial (CDTI) in Spain with aims at providing global surface soil moisture maps at a spatial resolution better than 50 km and a repeat cycle of less than 3 days with an accuracy of  $0.04 \text{ m}^3\cdot\text{m}^{-3}$  (Kerr et al., 2012). Recently, global soil moisture products, commonly named SMOS level 3 (L3 SM), at various temporal resolutions (daily products, 3-day composite products, 10-day aggregated products and monthly averaged products) have been made freely available by Central Aval de Traitment des Donnees (<http://catds.ifremer.fr>). The L3 products are filtered data in NetCDF format projected to the Equal-Area Scalable Earth (EASE) grid with spatial resolution of approximately  $25 \times 25 \text{ km}$  (Kerr et al., 2013). The main principal of the L3 processor is similar to the soil moisture level 2 processor, whereby from the multi-angular observed brightness temperatures (TB) are used to derive simultaneously soil moisture, optical thickness and other geophysical parameters by iteratively minimizing a cost function that is constructed from quadratic differences between the observed TB and computed TB (Kerr et al., 2013; Al-Yaarimet al., 2014). The main differences between L2 and L3 processors are the fact that the L3 processor considers several revisits simultaneously in a multi-orbital retrieval for each grid node, while the L2 processor just take in to account a single SMOS ascending or descending overpass to retrieve geophysical parameters (Kerr et al., 2013).Figure 2 demonstrates a sketch of SM L3 processing overview.

The L3 daily products include event detection flags (flood, freezing, snow, etc.) which deduced from time series analysis of SMOS and ancillary data. The events can be discovered if only the period of characteristic time of event is longer than SMOS revisit time. For the moment, only freezing events are applied to daily products(Kerr et al., 2013). The SMOS L3 data product (V2.7.1) from 2010 till 2015 that has been released since 01/03/2014 is used for presented study.

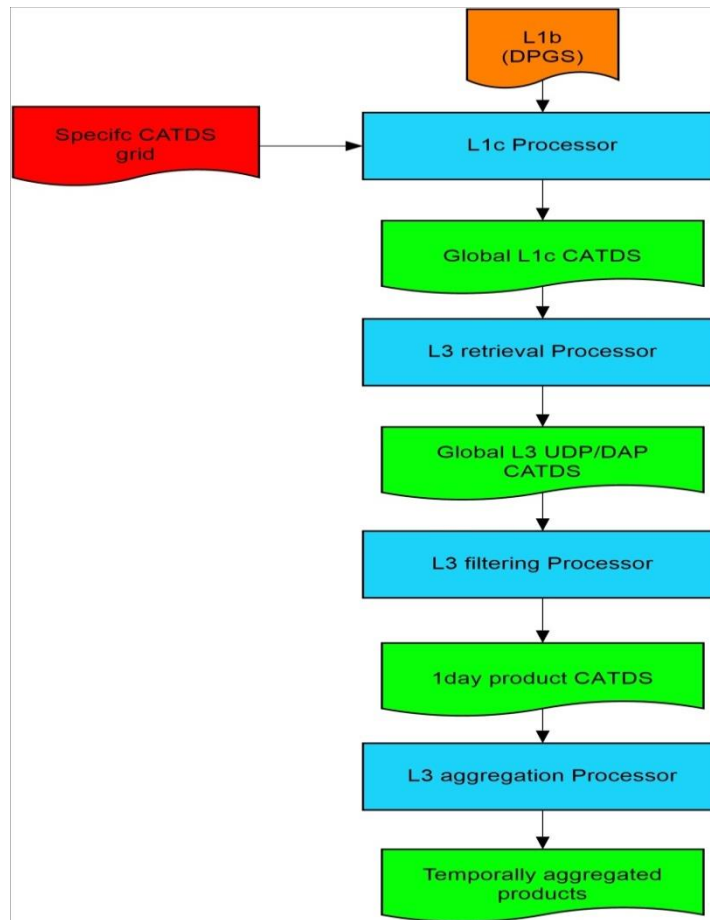


Figure 2: The schematic overview of processing L3 SM (Kerr et al., 2014).

### 3.1.2. SMAP radiometer soil moisture product level 2 (L2\_SM\_P)

The SMAP mission is managed by NASA's Jet Propulsion Laboratory and the satellite is placed into near polar sun-synchronous 6 AM/6 PM fixed orbit at an altitude of 685 Km and 8-day repeat cycle (Entekhabi et al., 2014). SMAP radiometer soil moisture product level 2 (L2\_SM\_P) is used for this study, which provides soil moisture content estimated from observed brightness temperature in half orbit on a fixed 36 km spatial resolution at Equal-Area Scalable Earth-2 (EASE2) grid. The target accuracy of SMAP L2\_SM\_P product is better than 0.04 ( $\text{m}^3 \text{m}^{-3}$ ) excluding regions with the presence of snow and ice, frozen ground, mountainous topography, open water, urban areas, and vegetation with water content greater than 5  $\text{kg m}^{-2}$  (Entekhabi et al., 2014). This science data product is available in the Hierarchical Data Format version 5 (HDF-5) and freely accessible in the public on National Snow and Ice data Center (NSISC) (<https://nsidc.org/data/smap>) with a 24 hours latency (Entekhabi et al., 2014).

The baseline retrieval algorithms for both SMOS and SMAP are based on the so-called tau-omega model (Entekhabi et al., 2014). The approach, however, adopted for estimating soil moisture is quite different. SMOS exploits capability of multi-angular observations to retrieve soil moisture, while SMAP utilizes the constant angle and complementary information such as open water fraction and frozen ground, provided

by radar instrument (Miernecki et al., 2014). In addition to radar information, which is known as a primary supplementary source of information, various static and dynamic ancillary data from other sources such as water information from the MODIS products and temperature information from GMAO model (GSFC Global Modelling & Assimilation Office) are employed in order to retrieve soil moisture reliably (Entekhabi et al., 2014).

The SMAP L2-SM-P includes two 16-bit data flags, surface flag and retrieval quality flag, which basically provide information about surface conditions of grid cell and the quality of soil moisture estimate when retrieval is attempted. For each individual grid cell, surface condition is numerically compared with two non-negative thresholds,  $T_1$  and  $T_2$ , where  $T_1 < T_2$ . For instance, in open water flag  $T_1$  is equal to 0.05 and  $T_2$  is considered 0.5 fraction of water for each cell. Retrieval soil moisture is attempted when surface condition situated below  $T_1$  or between  $T_1$  and  $T_2$ , while the grid cell is flagged for recommended quality and uncertain quality, respectively. For surface condition above  $T_2$  retrieval skipped (Entekhabi et al., 2014; O'Neill et al., 2015). Figure 3 shows simplified processing flow used to produce the SMAP L2-SM-P product.

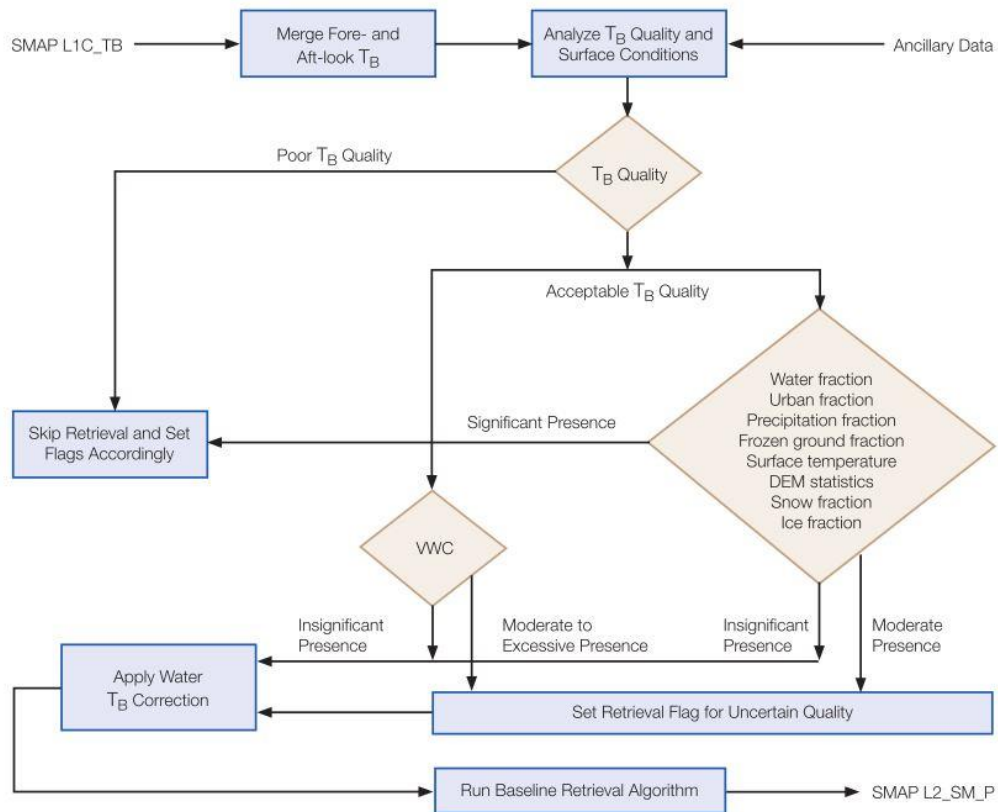


Figure 3, simplified schematic processing flow of SMAP L2-SM-P (Entekhabi et al., 2014)

### 3.2. Land Hydrological Model (LHM) soil moisture simulation

LHM is an operational, multi-scale, multi-model system for integrated water management, climate change and policy analysis developed jointly by Dutch hydrological institutes Alterra, Deltares, Netherlands Environmental Assessment Agency and RWS Waterdienst with a main goal of simulating the complete interaction hydrological system on national scale. Several national databases are supporting data for LHM, including subsoil, topsoil, land use, groundwater abstraction, drainage, water distribution, meteorological, topographical, vegetation development, vegetation-atmosphere and groundwater-surface water interaction (Delsman et al., 2008).

A main task of the LHM model is to help policy maker to optimize water distribution at national and regional levels in the Netherlands. To perform the goal several models are manipulated consisting of, Water model for Optimized Distribution (SWOD), which consider national and majority of regional surface water system, Surface Water model Sub-Catchment (SWSC) that is employed to derive water availability and demand from hinterland and Surface Water Flow and Transport (SWFT) that compute changes in the salt concentration and temperature distribution of the surface water. In addition, Soil Vegetation Atmosphere model for the Transfer of water (SVAT) and Groundwater (GW) model are used to simulate sub-surface water flow (De Lange et al., 2014).

The SVAT model consists of  $1300 \times 1200$  units for the entire Netherlands at a horizontal resolution of  $250 \times 250$  m. Only units that cover the study area are employed for this study. For each unit the model estimates the vertical transfers of water in column between saturated groundwater and the atmosphere either with root zone or with vegetation, which demonstrates importance of specification for dominate land-use at each SVAT-unit. The subsurface soil water dynamics for each unit is separated to two boxes, the root zone (shallow subsoil) and deep subsoil. Then for every unit, water balance and simulation are computed Eventually, two optional input files *FCWP\_SVAT.INP* and *GXG\_GG\_SVAT.INP* are used to generate information about root zone water content at field capacity and wilting point (P. E. V van Walsum, 2015)

## 4. METHOD

### 4.1. Upscaling strategies

The rationale for upscaling point measurements to coarse-scale is to provide information for a specific domain that might increase the confidence in calibration and validation of remotely sensed soil moisture data by reducing the spatial scale mismatch error. Various upscaling methods have been proposed for aggregation of in situ measurements to the satellite footprint. The general concept of all upscaling approaches can be mathematically formulated as,

$$\theta_{Domain} = F_{\uparrow}(\theta_{Point}) \quad (1)$$

where,  $\theta_{Point}$  is a vector that holds all point measurements,  $\theta_{Domain}$  stands for the soil moisture aggregated to the target domain, and  $F_{\uparrow}(\cdot)$  represents an arbitrary upscaling function (Crow et al., 2012).

Various approaches have been suggested for developing an upscaling function such as simple averaging, block kriging, hydrologic model-based and apparent thermal inertial (ATI) based methods (Qin et al., 2015). In this study simple averaging and a technique based on the output of a hydrologic model have been employed. Both are described in more detail below.

#### 4.1.1. Simple averaging

The first implemented approach for upscaling point scale soil moisture measurements is simple averaging, which can be formulated as,

$$\theta_{Upscale} = \frac{1}{N} \sum_{i=1}^N \theta_i^{Point} \quad (2)$$

where, the  $N$  represents the number of stations. The main assumption of this method is that the arithmetic mean of a limited number of individual realization is as a representative for the study area (Qin et al., 2015).

#### 4.1.2. Enhanced upscaling using distributed land surface modelling

Land surface models can be used as extra information to boost upscaling procedure when limited numbers of stations are available. However, the basic assumption is based on that the spatial soil moisture distribution simulated by the model is equivalent to distribution that would have been obtained when only *in-situ* measurements would have been used. Then, the up-scaling function can be developed from the relationship between mean of the soil moisture simulated at the pixels within which the monitoring stations are located ( $\bar{\theta}_{pixel}$ ) and mean of the soil moisture simulated across the either study domain ( $\theta_{domain}$ ), which is expressed by,

$$\theta_{Domain} = a * \bar{\theta}_{pixel} + b \quad (3)$$

where,  $a$  and  $b$  are the regression coefficients ( $m^3 m^{-3}$ ).

Since absolute soil moisture model simulations are sensitive to uncertainty following from the adopted parameterizations, it is likely to have different mean and dynamic range compared to *in-situ* soil moisture measurements. Therefore, to upscale mean *in-situ* measurement with derived regression coefficients mean and dynamic range of average *in-situ* measurements need to be corrected for these biases in the climatology between the two data sources.

In this research a bias correction approach is adopted that matches the first two statistical moments (mean and standard deviation) of the two data sets. In other words, the linear rescaling not only reduces the bias between the two datasets to near zero but also constrains the variance (Kornelsen & Coulibaly, 2015). This linear rescaling can be formulated as:

$$\bar{\theta}_{point}^{cor} = \frac{\sigma_{pixel}}{\sigma_{point}} (\bar{\theta}_{point} + b) \quad (4)$$

where,  $\bar{\theta}_{point}^{cor}$  is the bias corrected mean *in-situ* soil moisture measurement derived from  $\bar{\theta}_{point}$ ,  $b$  is bias between averaged soil moisture simulated at measurement location and averaged *in-situ* measurement datasets,  $\sigma_{pixel}$ ,  $\sigma_{point}$  are standard deviation of averaged simulated soil moisture at measurement location and standard deviation of averaged *in-situ* soil moisture dataset, respectively. When  $\bar{\theta}_{point}^{cor}$  is determined, then *in-situ* upscaled soil moisture ( $\theta_{Upscale}^{point}$ ) can be calculated with equation (3).

Finally, representative soil moisture of Twente region ( $\bar{\theta}_{Domain}^{point}$ ) could be estimated by reconverting  $\bar{\theta}_{upscaled}^{point}$  to temporal dynamics range of  $\bar{\theta}_{point}$ , which can be written as:

$$\bar{\theta}_{Domain}^{point} = \frac{\sigma_{point}}{\sigma_{pixel}} (\bar{\theta}_{upscaled}^{point} - b) \quad (5)$$

#### 4.2. Assessment metrics

For all the stations, statistical variables are computed from pair of the spatially distribution soil moisture products and the *in-situ* measurements. The mean difference (bias), the root mean square difference (RMSD), correlation coefficient (R) and normalized standard deviation are considered. These variables can be calculated as follows (Al-Yaari et al., 2014; Kornelsen & Coulibaly, 2015; Albergel et al., 2012)

$$Bias = \mu_Y - \mu_X \quad (6)$$

$$R = \left( \frac{Cov(Y, X)}{\sigma_Y \sigma_X} \right) \quad (7)$$

$$RMSD = \left( \frac{1}{N} \sum_{i=0}^N (Y - X)^2 \right)^{1/2} \quad (8)$$

$$\hat{\sigma} = \frac{\sigma_X}{\sigma_Y} \quad (9)$$

where,  $X$  is distributed surface soil moisture dataset and  $Y$  is the referenced dataset,  $\mu$  is temporal mean,  $\sigma$  is standard deviation,  $Cov(\cdot)$  is the covariance between the datasets and  $N$  the number of samples.

In addition, to separate the differences in patterns and means of the two datasets, normalized centred root mean squared difference (E) between simulated products and *in-situ* are calculated (Taylor, 2001),

$$E^2 = \hat{\sigma}^2 + 1 - 2\hat{\sigma}R \quad (10)$$

Taylor diagram can be employed to statistically quantify the degree of similarity between the two datasets (Taylor, 2001). On the diagram correlation coefficient, centred root mean squared differences and normalized standard deviation are summarized in a single point in a two dimensional plot. Radial distance from the origin displays the normalized standard deviation and the angle in the polar plot represents the correlation with referenced data. Reference dataset is located on the x axis at R=1 and  $\hat{\sigma}^2=1$  and distance from this point represents the centred normalized root mean squared differences (E) between the two datasets.

## 5. Model-based up-scaling

Point measurements are only representative of measurement locations and not necessarily support coarse-resolution satellite observation because of heterogeneity of soil and vegetation cover (Bircher et al.,2012). Therefore, direct comparison of *in-situ* measurements with coarse-scaled microwave remotely sensed products may not be robust enough. Simple averaging and up-scaling based on the model simulated soil moisture strategies are selected in this research to efficiently translate sparse point measurements to the satellite foot prints.

For the model-based up-scaling method, quality of simulated products needs to be assessed before the model is employed for the development of the up-scaling function, since simulated products are likely to be influenced by systematic differences in comparison to *in-situ* measurements.

### 5.1. Time series analysis

As such the first step is to investigate the reliability of the available LHM data against *in-situ* measurements. Time series analysis between simulated product at measurement locations and individual *in-situ* measurements for 5 cm layer depth along with daily precipitation for the year 2012 are presented in Figure 4(time series analysis for 2013 and 2014 are presented in Figure 16 and Figure 17, respectively).

In general, the LHM simulated soil moisture captures the temporal dynamics of measurements collected by the monitoring stations. For instance in Julian day 235 with extensive rainfall *in-situ* and simulated product present sharp increases in soil moisture value. However, systematic differences can be noted in the mean and the soil moisture change in response to rainfall. Probable reasons for the biases and reactivity of LHM product can be explained by, either sensitivity of the land surface model to uncertainty from adapted parameterization or overestimation of soil moisture content by the Probe measurements at 5 cm depth .Very high value of soil moisture measurements at stations 6, 18 in year 2013 and 4, 6 for year 2014 are observed. Moreover, spatial scale differences between two datasets and different depth of simulation and measurements of soil moisture can be another caused of the variation between the two datasets. LHM provides soil moisture simulation at column of root zone which is various from 30 cm to 1 m depth, while soil moisture is measured at 5 cm depth.

In addition, the statistical scores of the comparison in terms of correlation coefficient (R), root mean squared differences (RMSD) and biases between the two datasets in years 2012, 2013 and 2014 are presented in Table 1. The range of correlation values between individual *in-situ* measurements and LHM simulated product at monitoring locations varies from -0.60 to 0.86, -0.66 to 0.82 and -0.45 to 0.77 with mean correlation values of 0.17, 0.28 and 0.03 for 2012, 2013 and 2014 respectively. On average, station 17 presents the best correlation value with average value of 0.70, while stations 3 and 7 demonstrate the highest negative value with average of -0.51.

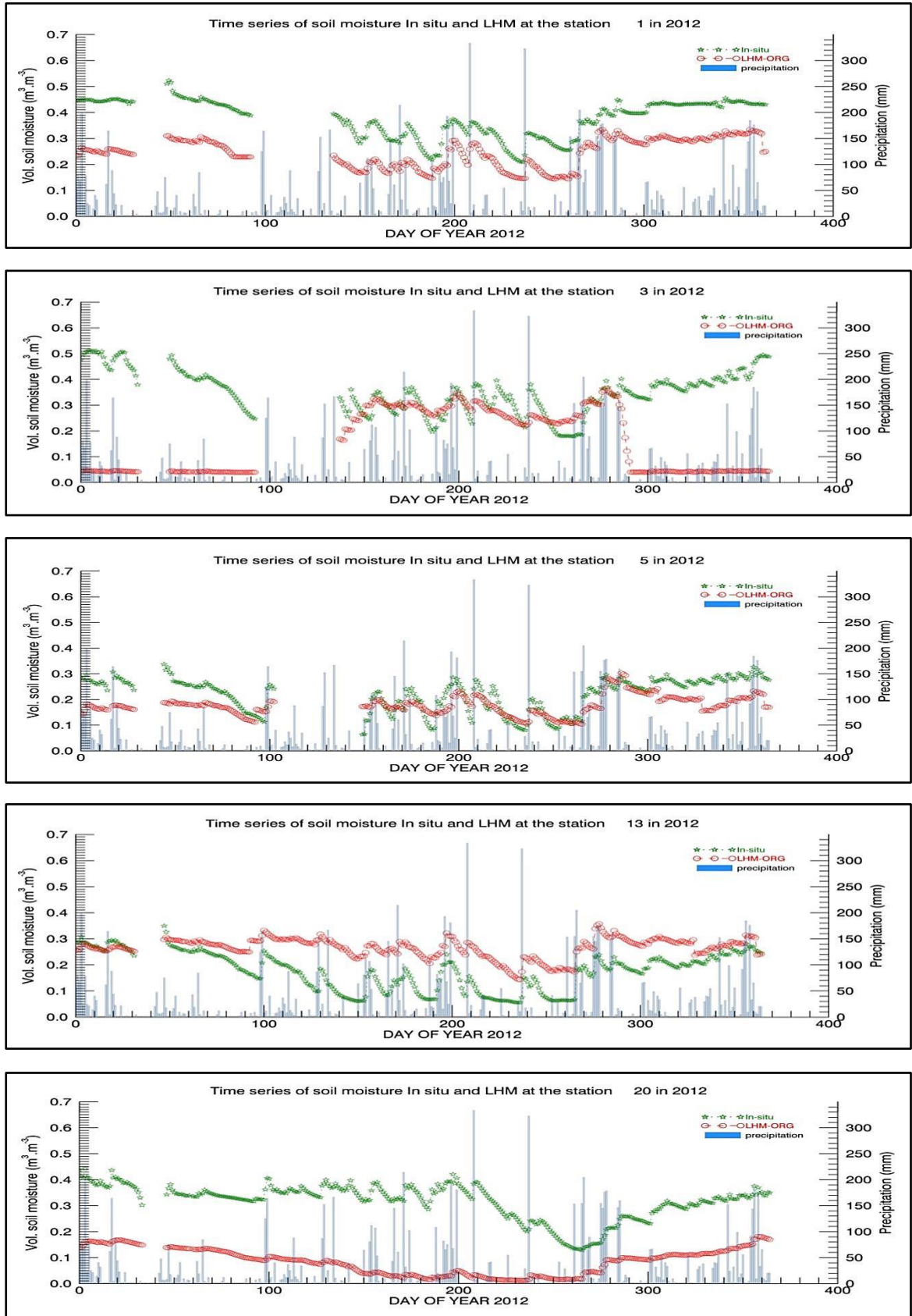


Figure 4, temporal evaluation of individual *in-situ* measurements and simulated surface soil moisture in measurement locations along with daily rainfall in 2012 are presented

Table 1, Pearson correlation(R), root mean squared differences (RMSD) and bias between individual station measurements and original LHM product for 2012, 2013 and 2014 are presented.

station	R				Bias (m <sup>3</sup> .m <sup>-3</sup> )				RMSD (m <sup>3</sup> .m <sup>-3</sup> )			
	2012	2013	2014	Average	2012	2013	2014	Average	2012	2013	2014	Average
1	0.86	0.82	-0.19	0.50	-0.13	-0.12	0.00	-0.08	0.14	0.13	0.13	0.13
2	0.59	0.50	0.30	0.46	-0.01	-0.05	-0.10	-0.05	0.07	0.07	0.12	0.09
3	-0.60	-0.66	-0.26	-0.51	-0.19	-0.16	-0.19	-0.18	0.26	0.26	0.24	0.25
4	0.40	0.77	0.43	0.53	-0.16	-0.23	-0.24	-0.21	0.21	0.26	0.26	0.25
5	0.67	0.57	0.19	0.48	-0.04	-0.04	-0.06	-0.05	0.06	0.07	0.08	0.07
6	-0.25	0.86	0.11	0.24	-0.09	-0.05	-0.17	-0.10	0.13	0.11	0.18	0.14
7	-0.45	-0.65	-0.41	-0.51	-0.09	-0.07	-0.03	-0.06	0.17	0.19	0.15	0.17
8	-0.19	-0.25	-0.29	-0.24	-0.13	-0.03	-0.09	-0.08	0.17	0.12	0.13	0.14
9	0.56	0.48	0.18	0.41	-0.02	-0.01	-0.01	-0.01	0.06	0.07	0.05	0.06
10	0.13	-0.47	0.12	-0.07	-0.10	-0.17	0.27	0.00	0.12	0.17	0.27	0.19
11	0.38	0.65	0.48	0.50	-0.11	-0.09	-0.10	-0.10	0.12	0.10	0.10	0.11
12	-0.29	0.23	-0.29	-0.12	0.10	0.06	0.08	0.08	0.14	0.11	0.14	0.13
13	0.66	0.65	0.35	0.55	0.09	0.10	0.12	0.10	0.10	0.11	0.13	0.11
14	-0.15		-0.45	-0.30	-0.17	-	-0.03	-0.10	0.18	-	0.04	0.11
15	-0.44	0.34	-0.25	-0.12	-0.06	0.03	-0.05	-0.03	0.12	0.09	0.09	0.10
16	-	-0.12	-0.05	-0.09	-	0.05	0.07	0.06	-	0.08	0.10	0.09
17	0.76	0.63	-	0.70	0.11	0.09	-	0.10	0.12	0.10	-	0.11
18	-0.08	0.40	-0.21	0.04	-0.11	-0.08	-0.05	-0.08	0.15	0.13	0.11	0.13
19	0.15	0.35	0.05	0.18	0.06	0.06	0.01	0.04	0.10	0.09	0.04	0.08
20	0.44	0.43	0.77	0.55	-0.23	-0.16	-0.10	-0.16	0.24	0.18	0.11	0.17
<b>Average</b>	0.17	0.29	0.03	0.16	-0.07	-0.05	-0.04	-0.05	0.14	0.13	0.13	0.13

Although, the modelled product follows the temporal dynamics of *in-situ* dataset, a particular underestimation can be observed specifically in station 20. Annually, mean dry biases of  $-0.07 \text{ m}^3.\text{m}^{-3}$ ,  $-0.05 \text{ m}^3.\text{m}^{-3}$  and  $-0.04 \text{ m}^3.\text{m}^{-3}$  are monitored for years 2012, 2013 and 2014 respectively. Station 4 with averaged value of  $-0.21 \text{ m}^3.\text{m}^{-3}$  presents the highest negative biases, whereas, minimum systematic differences are observed for station 9 with mean value of  $-0.01 \text{ m}^3.\text{m}^{-3}$ . In terms of RMSD, the mean values for 3 years are almost equal with  $0.14 \text{ m}^3.\text{m}^{-3}$ ,  $0.13 \text{ m}^3.\text{m}^{-3}$  and  $0.13 \text{ m}^3.\text{m}^{-3}$  for 2012, 2013 and 2014 respectively. The highest averaged RMSD is monitored for both stations 3 and 4 with mean of  $0.25 \text{ m}^3.\text{m}^{-3}$  while station 9 shows the lowest RMSD with three years average of  $0.06 \text{ m}^3.\text{m}^{-3}$ . Since the RMSD consist of biases and centred RMSD, possible reason for high and low monitored RMSD in stations 4 and 9 can be the effect of biases.

Although, LHM product generally follows the temporal trends of in-situ measurements, in some stations spatially stations 3, 7 and 8 the simulated seasonal soil moisture variability is not appropriately reproduced by the LHM. In the winter the LHM soil moisture does not become wetter as is expected, but presents drier. Nevertheless the soil moisture dynamics simulated for the summer period capture the measurements and fluctuate in response to precipitation input better. Consequently, since winter period is not sufficiently

reliable the summer period (Julian day from 152 to 282) was selected for developing the up-scaling function.

Statistical results of comparison between simulated product at measurement location and in-situ measurements in the summer period for years 2012, 2013 and 2014 are given in Table 2. On average for all the stations, mean correlation value of 0.68, 0.68 and 0.65 for the years 2012, 2013 and 2014 are observed, which illustrates significant increases in terms of correlation values compared to annual period. LHM product presents slightly wet biases with mean values  $0.02 \text{ m}^3.\text{m}^{-3}$  and  $0.03 \text{ m}^3.\text{m}^{-3}$  for years 2013 and 2014, respectively.

Table 2 presents statistical results of comparison between *in-situ* measurements and LHM product in summer period of years 2012, 2013 and 2014.

station	R				Bias ( $\text{m}^3 \text{m}^{-3}$ )				RMSD ( $\text{m}^3.\text{m}^{-3}$ )			
	2012	2013	2014	average	2012	2013	2014	average	2012	2013	2014	average
1	0.87	0.92	0.90	0.90	-0.11	-0.08	0.08	-0.03	0.11	0.08	0.09	0.09
2	0.74	0.78	-	0.76	0.04	-0.01	-	0.01	0.05	0.04	-	0.05
3	0.65	0.83	-	0.74	-0.01	0.07	-	0.03	0.05	0.08	-	0.06
4	0.14	0.93	0.48	0.52	-0.06	-0.12	-0.15	-0.11	0.09	0.12	0.15	0.12
5	0.80	0.83	0.52	0.72	-0.01	0.01	-0.01	0.00	0.04	0.04	0.05	0.04
6	0.83	0.83	0.84	0.83	-0.03	0.02	-0.15	-0.05	0.06	0.05	0.15	0.09
7	0.32	0.77	0.85	0.65	0.06	0.15	0.14	0.12	0.08	0.15	0.14	0.12
8	0.84	0.37	0.72	0.65	-0.03	0.08	0.03	0.03	0.04	0.12	0.04	0.07
9	0.72	0.74	0.63	0.70	-0.01	0.03	0.04	0.02	0.06	0.06	0.05	0.06
10	0.86	-	0.81	0.83	-0.07	-	0.26	0.10	0.07	-	0.26	0.17
11	0.69	0.74	0.51	0.65	-0.08	-0.08	-0.08	-0.08	0.09	0.10	0.09	0.09
12	0.86	0.88	0.65	0.80	0.16	0.12	0.13	0.14	0.17	0.13	0.15	0.15
13	0.87	0.79	0.87	0.84	0.12	0.12	0.14	0.13	0.13	0.13	0.14	0.13
14	-	-	-	-	-	-	-	-	-	-	-	-
15	0.79	0.94	0.53	0.75	0.02	0.08	0.00	0.03	0.04	0.08	0.03	0.05
16	-	-	-	-	-	-	-	-	-	-	-	-
17	0.80	0.34	-	0.57	0.11	0.06	-	0.08	0.11	0.09	-	0.10
18	0.76	0.70	0.45	0.64	-0.04	0.00	0.04	0.00	0.06	0.04	0.06	0.06
19	0.67	0.39	0.35	0.47	0.12	0.11	0.00	0.08	0.12	0.12	0.02	0.09
20	0.01	-0.25	0.59	0.12	-0.25	-0.15	-0.10	-0.17	0.26	0.17	0.10	0.18
Average	0.68	0.68	0.65	0.67	0.00	0.02	0.03	0.02	0.09	0.09	0.10	0.10

## 5.2. Taylor diagram

Taylor diagram offers excellent graphically demonstration of three different statistic ( $R$ ,  $E$ ,  $\hat{\sigma}$ ) on two dimensional plot. These statistics together provide quick summery of how accurately model simulated the natural system(Taylor, 2001).Therefore, the diagram is employed to assess the reliability of simulated product without interference of the bias in wet and dry seasons separately due to different performances of LHM in these periods.

Six Taylor diagrams displaying the measure of differences among LHM product at measurement locations in summer period and yearly against *in-situ* observation for years 2012, 2013 and 2014 are presented in Figure 5. The diagrams are only illustrating stations with positive correlation between two datasets. As such, stations 3, 6, 7, 8, 12, 14, 15 and 18, stations 3, 7, 8, 10 and 16 and stations 1, 3, 7, 8, 12, 14, 15, 16, 18 are excluded for years 2012, 2013 and 2014, respectively.

In general for annual comparison, the diagrams highlight almost good range of correlation for years 2012 and 2013 with most values are observed between 0.5 and 0.75, while correlation values for majority of stations in year 2014 were extremely low and monitored below 0.3, which indicated a poor linear relationship between the two datasets and LHM spatially distributed product cannot be able properly simulate the *in-situ* measurements collected by individual stations. In addition, for years 2012 and 2013 station symbols showed smaller dispersion compare to year 2014, which can be described by smaller range of correlation values and closer standard deviation of simulated products to in situ measurements in these years.

Moreover, for majority of stations dynamic ranges of simulated soil moisture were estimated lower than the *in-situ* measurement, which lead to station symbols mostly are presenting below the line of normalized standard deviation one. However, station 17 presents a quit high normalize standard deviation in year 2013

In the summer period (Julian day from 152 to 282) the diagrams underline significant increases of correlation values between simulated product and in-situ measurements for years 2012 and 2013. Most correlation values were observed between 0.7 to 0.9 and 0.75 to 0.95 for year 2012 and 2013, respectively. However, the range of correlation values monitored for 2014 were between 0.35 and 0.85.

In the summer period, more station symbols are presenting above the line of normalized standard deviation 1 in comparison to yearly diagrams, which indicates the variability of simulated soil moisture in the this period is higher than annuals respect to *in-situ* measurements. Moreover, in this period, stations are demonstrating larger dispersion especially for year 2013 in comparison of annuals diagrams.

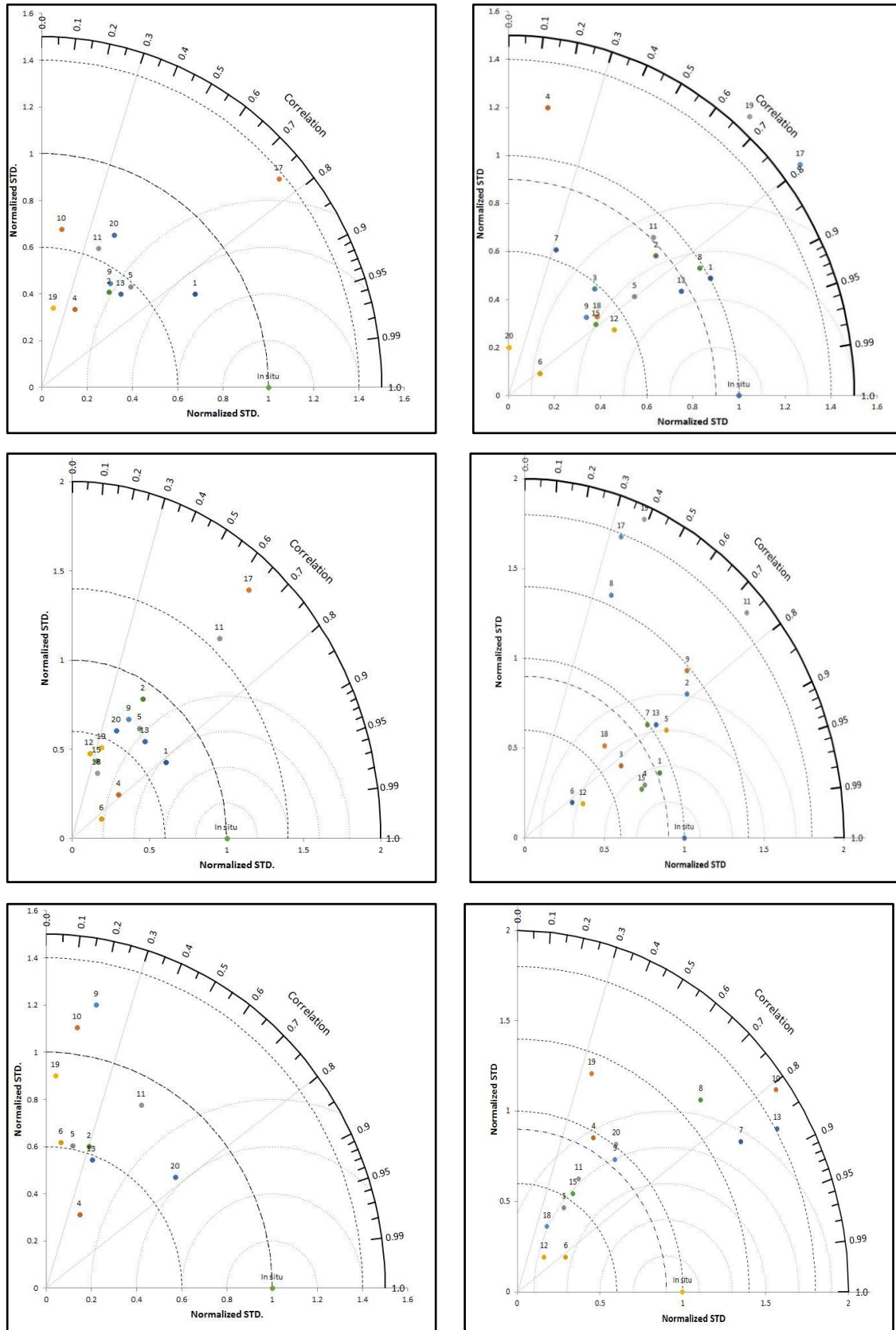


Figure 5, presents Taylor diagrams demonstrating results of comparison among individual *in-situ* measurements, annual (left) and summer (right) simulated product at measurements location for 2012 (top), 2013 (middle) and 2014 (bottom). Only stations with positive correlation are presented.

### 5.3. Soil moisture aggregated across the study domain

The time series of averaged simulated soil moisture at measurement locations ( $\bar{\theta}_{pixel}$ ) and spatially averaged simulated soil moisture over the whole domain ( $\theta_{Domain}$ ) for years 2012, 2013 and 2014 are presented in Figure 6. Since *in-situ* measurements were influenced by an equipment malfunction and all stations did not provide data for the entire summer period, then some stations are excluded for calculating mean *in-situ* measurement ( $\bar{\theta}_{point}$ ). As a result,  $\bar{\theta}_{pixel}$  include different stations for each year. As such, stations 6, 14, 15, 16, and 18 for the year 2012, stations, 10, 14 and 16 for the year 2013 and stations 1, 2, 3, 5, 10, 13, 14, 16, 17, 19 for the year 2014 are excluded.

Statistical results of comparison between  $\bar{\theta}_{pixel}$  and  $\theta_{Domain}$  are presented in Table 3. In general,  $\bar{\theta}_{pixel}$  captures temporal variation of  $\theta_{Domain}$  quiet well, However, systematic differences are found in the means of datasets. In terms of correlation, two datasets presents strong linear relationship with correlation values of 0.98, 0.99 and 0.95 for 2012, 2013 and 2014, respectively. Negative biases of  $-0.03 \text{ m}^3.\text{m}^{-3}$ ,  $-0.02 \text{ m}^3.\text{m}^{-3}$  and  $-0.03 \text{ m}^3.\text{m}^{-3}$  are found for  $\bar{\theta}_{pixel}$  for all three years which leads to RMSD between two datasets.

Table 3 gives statistical result of comparison between simulated soil moisture at measurements location ( $\bar{\theta}_{pixel}$ ) and averaged simulated product over entire domain ( $\theta_{Domain}$ )

$\bar{\theta}_{pixel}$ Vs. $\theta_{Domain}$			
	R	Bias ( $\text{m}^3 \text{m}^{-3}$ )	RMSD ( $\text{m}^3 \text{m}^{-3}$ )
2012	0.98	-0.03	0.03
2013	0.99	-0.02	0.02
2014	0.95	-0.03	0.03

The correlation performances of  $\bar{\theta}_{pixel}$  and the bias corrected mean *in-situ* soil moisture measurement  $\bar{\theta}_{point}^{cor}$  are demonstrated in Figure 7. Strong linear relationship for years 2012, 2013 and almost equal dynamic range of soil moisture for the both products is monitored. However, lower correlation value and some outliers are observed in years 2014 and 2013, respectively. Statistical scores of comparison between two datasets for years 2012, 2013 and 2014 are given in Table 4. In terms of correlation, correlation values of 0.92, 0.90 and 0.80 are found for consecutive years. The highest dry biases of  $-0.03 \text{ m}^3.\text{m}^{-3}$  are found for  $\bar{\theta}_{pixel}$  respect to  $\bar{\theta}_{point}^{cor}$  in year 2013, which is caused the highest RMSD between two datasets, while in the year 2012 systematic differences in mean of two datasets is removed by the bias correction method.

Table 4 presents statistical result of comparison between simulated soil moisture at measurements location ( $\bar{\theta}_{pixel}$ ) and bias corrected mean *in-situ* soil moisture measurement ( $\bar{\theta}_{point}^{cor}$ ).

$\bar{\theta}_{pixel}$ Vs. $\bar{\theta}_{point}^{cor}$			
	R	Bias ( $m^3 m^{-3}$ )	RMSD ( $m^3 m^{-3}$ )
2012	0.92	0	0.02
2013	0.90	-0.03	0.04
2014	0.8	0.01	0.02

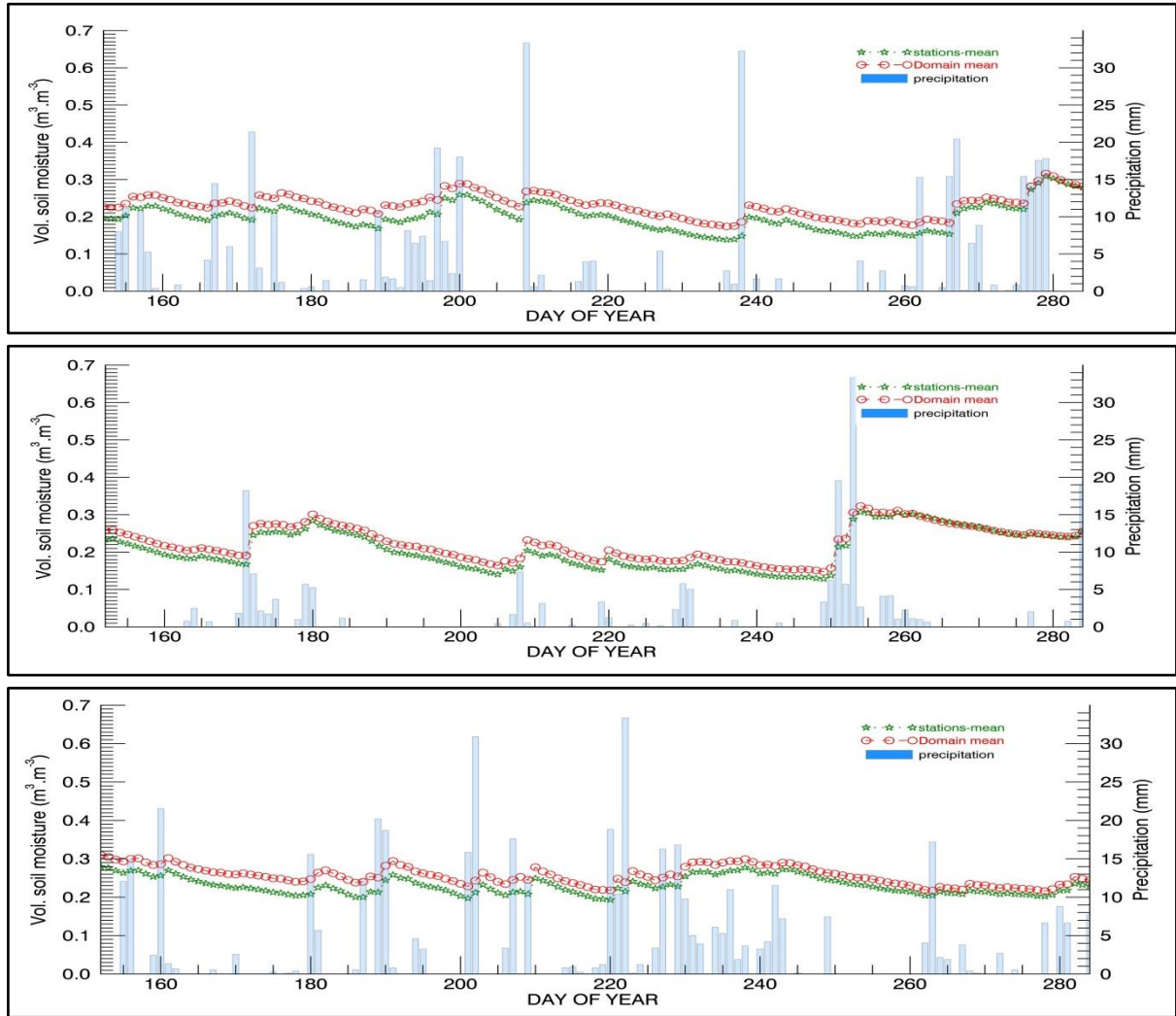


Figure 6 time series of the averaged simulated soil moisture at measurement locations along with spatially averaged over the whole domain and daily precipitation for 2012 (Top), 2013 (Middle) and 2014 (Bottom).

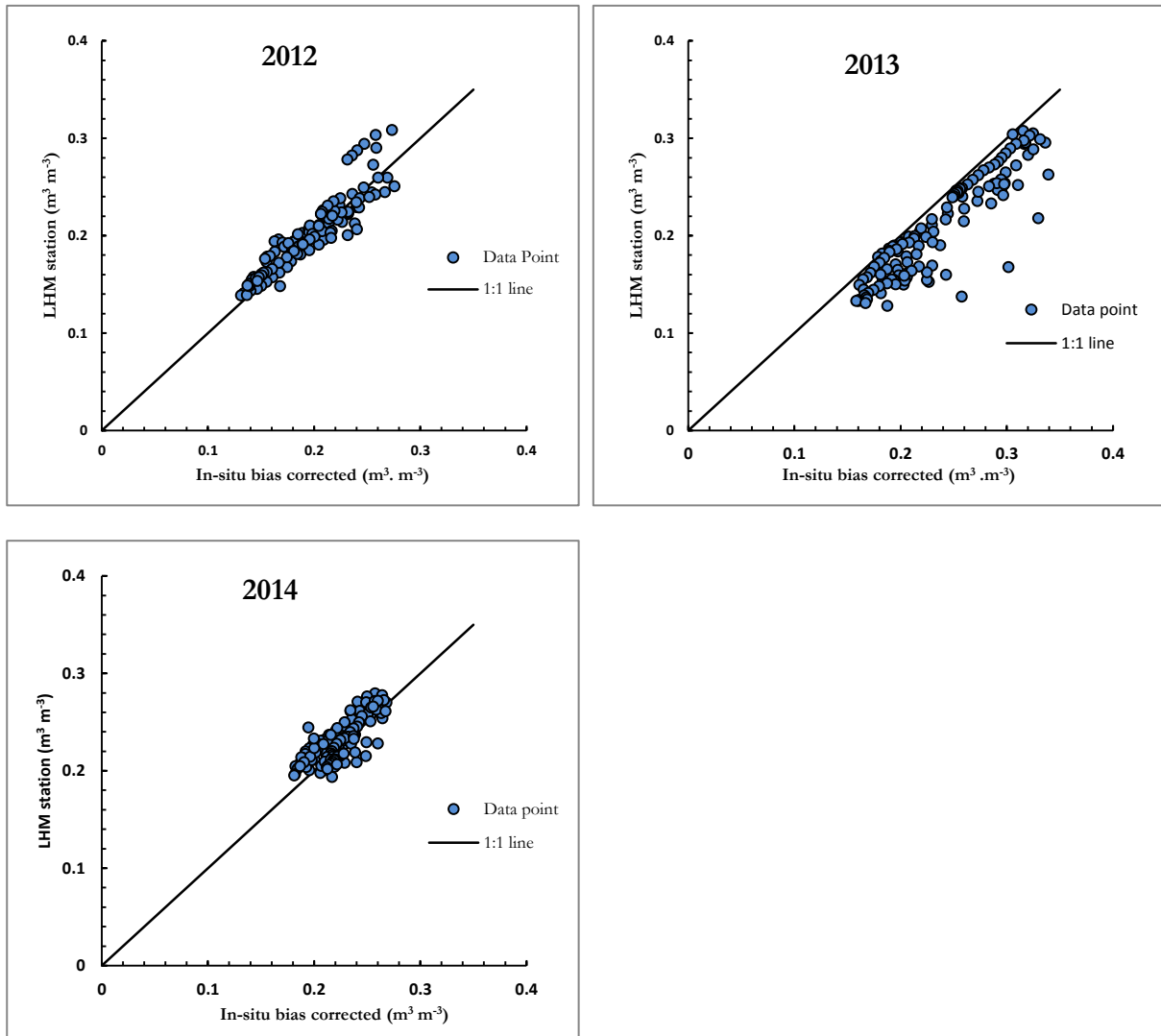


Figure 7 scatter plots of averaged simulated soil moisture at measurement locations (LHM station) and the bias corrected mean *in-situ* soil moisture measurement for the summer period of years 2012, 2013 and 2014.

#### 5.4. Upscaling functions

Linear regression between mean LHM at measurement location ( $\bar{\theta}_{pixel}$ ) and aggregated soil moisture for entire domain ( $\theta_{Domain}$ ) is established and considered as up-scaling function. Figure 8 presents scatter plots between  $\bar{\theta}_{pixel}$  and  $\theta_{Domain}$  for years 2012, 2013, 2014 and 2015. The scatter plots present strong linear relationship with almost equal range of soil moisture between two datasets. Since different stations are employed for calculation of  $\bar{\theta}_{pixel}$ , each year slightly differences in patterns of data point can be noted, which lead to meager variation in up-scaling parameters. Up-scaling parameters along with coefficient determination for datasets are given in Table 5. Since LHM data is not available for year 2015, *in-situ* measurements in year 2015 and simulated products in years 2012 and 2013 are manipulated to develop up-

scaling function for year 2015. LHM product in year 2014 is not considered due to lower correlation value respect to other years.

Table 5 presents slopes and intercepts of up-scaling functions along with coefficient determination between  $\bar{\theta}_{pixel}$  and  $\theta_{Domain}$  datasets for years 2012, 2013 and 2014.

	2012	2013	2014	2015
<b>a</b>	0.841	0.880	1.005	0.885
<b>b (m<sup>3</sup>.m<sup>-3</sup>)</b>	0.062	0.043	0.025	0.061
<b>R<sup>2</sup></b>	0.964	0.972	0.952	0.951

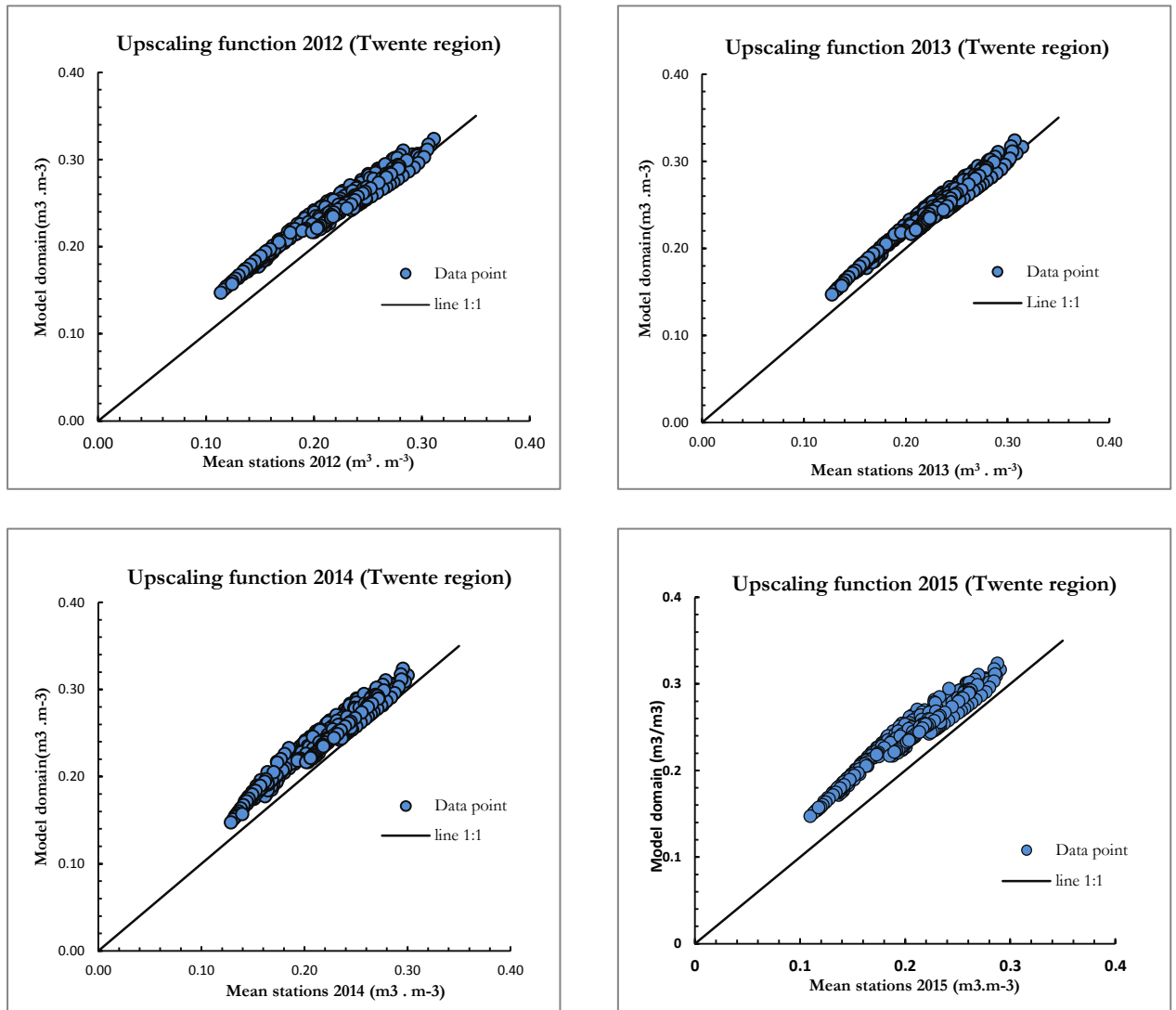


Figure 8 scatter plots of  $\bar{\theta}_{pixel}$  (stations) and  $\theta_{Domain}$ (model domain) and for years 2012, 2013, 2014 and 2015.

## 6. ASSESSMENT OF SATELLITE-BASED PRODUCTS

### 6.1. Comparison of individual stations with SMOS L3 SM

Seven pixels of original SMOS L3 SM obtained from the ascending overpass are directly compared to soil moisture measurement at individual stations for years 2010, 2011, 2012, 2013, 2014 and 2015. The results of the comparison in terms of correlation values, root mean squared differences and biases between two datasets are given in Table 6 and Table 7. The ranges of correlation values are observed between 0.46 - 0.72, 0.17 - 0.62, 0.3-0.61, 0 - 0.66, 0.22 - 0.62 and 0.14 - 0.67 with average values of 0.61, 0.39, 0.49, 0.50, 0.45 and 0.45 for consecutive years. On average, the highest correlation value is monitored for station 5 with average value of 0.57, while station 20 demonstrates the lowest value with average of 0.35, which can be explained by the location of the station and influence of dense vegetation on microwave signals. In general, continuous dry mean biases expect in year 2014 are found for the SMOS product. On average, the largest negative biases value for SMOS is monitored in 2012 with value of  $-0.11 \text{ m}^3\cdot\text{m}^{-3}$ , while for the year 2014 no biases between datasets are found. The highest negative systematic differences between SMOS product and individual measurements presents at station 10 with average value of  $-0.2 \text{ m}^3\cdot\text{m}^{-3}$  whereas, station 9 is observed as a non-bias station.

Table 6 Pearson correlation (R), root mean squared differences (RMSD) and bias between individual station measurements and SMOSL3 for 2010, 2011 and 2012

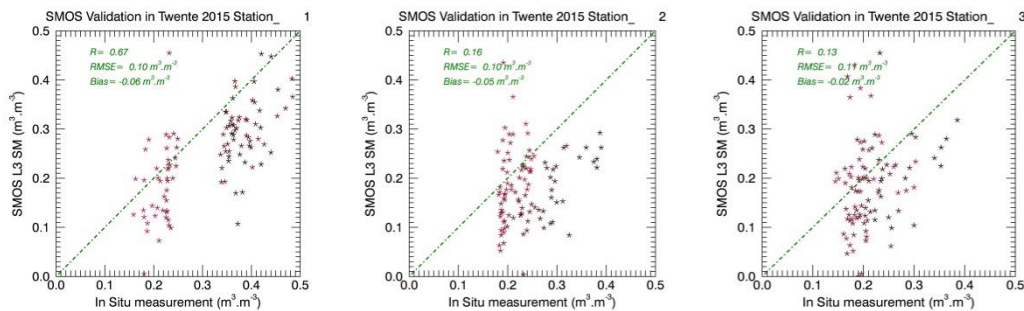
Station	2010			2011			2012		
	R	RMSD ( $\text{m}^3 \text{ m}^{-3}$ )	Bias ( $\text{m}^3\cdot\text{m}^{-3}$ )	R	RMSD ( $\text{m}^3 \text{ m}^{-3}$ )	Bias ( $\text{m}^3\cdot\text{m}^{-3}$ )	R	RMSD ( $\text{m}^3\cdot\text{m}^{-3}$ )	Bias ( $\text{m}^3\cdot\text{m}^{-3}$ )
1	0.47	0.19	-0.17	0.20	0.22	-0.19	0.42	0.24	-0.22
2	0.71	0.07	0.03	0.33	0.12	0.05	0.52	0.10	-0.02
3	0.66	0.19	-0.18	0.52	0.15	-0.11	0.58	0.21	-0.19
4	0.53	0.19	-0.16	0.42	0.19	-0.14	0.61	0.17	-0.11
5	0.67	0.08	-0.04	0.55	0.09	-0.01	0.44	0.12	-0.05
6	0.62	0.10	-0.06	0.51	0.21	-0.18	-	-	-
7	0.50	0.09	-0.05	0.37	0.10	-0.03	0.30	0.13	-0.10
8	0.60	0.08	-0.01	0.52	0.08	-0.01	0.45	0.10	-0.05
9	0.62	0.08	-0.04	0.42	0.09	0.00	0.54	0.08	-0.02
10	0.46	0.23	-0.20	0.20	0.21	-0.17	0.51	0.23	-0.22
11	0.68	0.14	-0.11	0.44	0.12	-0.07	0.37	0.14	-0.11
12	0.72	0.07	-0.02	0.28	0.13	-0.06	0.42	0.15	-0.11
13	0.67	0.08	-0.03	0.33	0.11	0.03	0.36	0.10	-0.02
14	-	-	-	0.62	0.13	-0.09	-	-	-
15	0.60	0.17	-0.14	0.30	0.17	-0.10	0.61	0.14	-0.11
16	0.58	0.16	-0.14	-	-	-	-	-	-
17	0.63	0.10	0.06	-	-	-	0.48	0.10	0.02
18	0.65	0.13	-0.05	0.56	0.15	-0.06	0.57	0.16	-0.11
19	0.59	0.14	-0.09	0.17	0.15	-0.03	0.58	0.11	-0.03
20	0.59	0.14	-0.11	0.32	0.08	-0.03	0.51	0.18	-0.14
average	<b>0.61</b>	<b>0.13</b>	<b>-0.08</b>	<b>0.39</b>	<b>0.14</b>	<b>-0.07</b>	<b>0.49</b>	<b>0.16</b>	<b>-0.11</b>

Table 7 Pearson correlation (R), root mean squared differences (RMSD) and bias between individual station measurements and SMOSL3 for 2013, 2014 and 2015

Station	2013			2014			2015		
	R	RMSD ( $\text{m}^3.\text{m}^{-3}$ )	Bias ( $\text{m}^3.\text{m}^{-3}$ )	R	RMSD ( $\text{m}^3.\text{m}^{-3}$ )	Bias ( $\text{m}^3.\text{m}^{-3}$ )	R	RMSD ( $\text{m}^3.\text{m}^{-3}$ )	Bias ( $\text{m}^3.\text{m}^{-3}$ )
1	0.41	0.19	-0.17	0.24	0.13	0.02	0.67	0.10	-0.06
2	0.61	0.08	-0.03	-	-	-	0.17	0.10	-0.05
3	0.50	0.14	-0.09	-	-	-	0.14	0.10	-0.02
4	0.62	0.19	-0.14	0.26	0.15	-0.08	0.52	0.17	-0.06
5	0.66	0.08	-0.02	0.62	0.07	0.02	0.49	0.12	0.04
6	-	-	-	0.48	0.30	-0.28	-	-	-
7	0.33	0.09	-0.02	0.36	0.11	0.07	0.57	0.11	-0.03
8	0.51	0.12	0.08	0.45	0.10	0.06	0.57	0.11	0.05
9	0.58	0.09	0.04	0.44	0.10	0.06	0.55	0.11	-0.04
10	-	-	-	-	-	-	-	-	-
11	0.62	0.09	-0.04	0.54	0.08	0.00	0.53	0.09	0.03
12	0.59	0.12	-0.09	0.52	0.09	-0.02	0.42	0.13	-0.01
13	0.54	0.09	0.04	0.55	0.12	0.10	0.62	0.11	0.06
14	-	-	-	-	-	-	0.35	0.12	-0.06
15	0.65	0.09	0.01	0.60	0.08	-0.03	0.51	0.08	-0.02
16	-	-	-	-	-	-	0.45	0.14	-0.06
17	0.57	0.14	0.10	-	-	-	-	-	-
18	0.57	0.11	-0.01	0.53	0.10	0.03	0.24	0.14	0.02
19	0.30	0.12	0.03	0.44	0.09	-0.04	-	-	-
20	0.00	0.14	-0.01	0.22	0.12	0.07	0.44	0.11	0.05
average	<b>0.50</b>	<b>0.13</b>	<b>-0.04</b>	<b>0.45</b>	<b>0.12</b>	<b>0.00</b>	<b>0.45</b>	<b>0.13</b>	<b>-0.03</b>

Very high negative biases for station 10 can be explained by the location of station that used to be near ditch and was changed in the year 2013. In terms of RMSD, very similar conclusion respect to biases can be drawn. On average, the highest value of RMSD is observed for SMOS in the year 2012 equal to  $0.16 \text{ m}^3.\text{m}^{-3}$ , while in year 2014, the lowest RMSD mean value ( $0.12 \text{ m}^3.\text{m}^{-3}$ ) is found for SMOS.

Scatter plots of the two product correlation performances are displayed in Figure 9. The scatters plots demonstrate overall underestimation of SMOS product and almost equal dynamic range of soil moisture for both products. However, in some stations such as 8 and 20 SMOS represents the higher range.



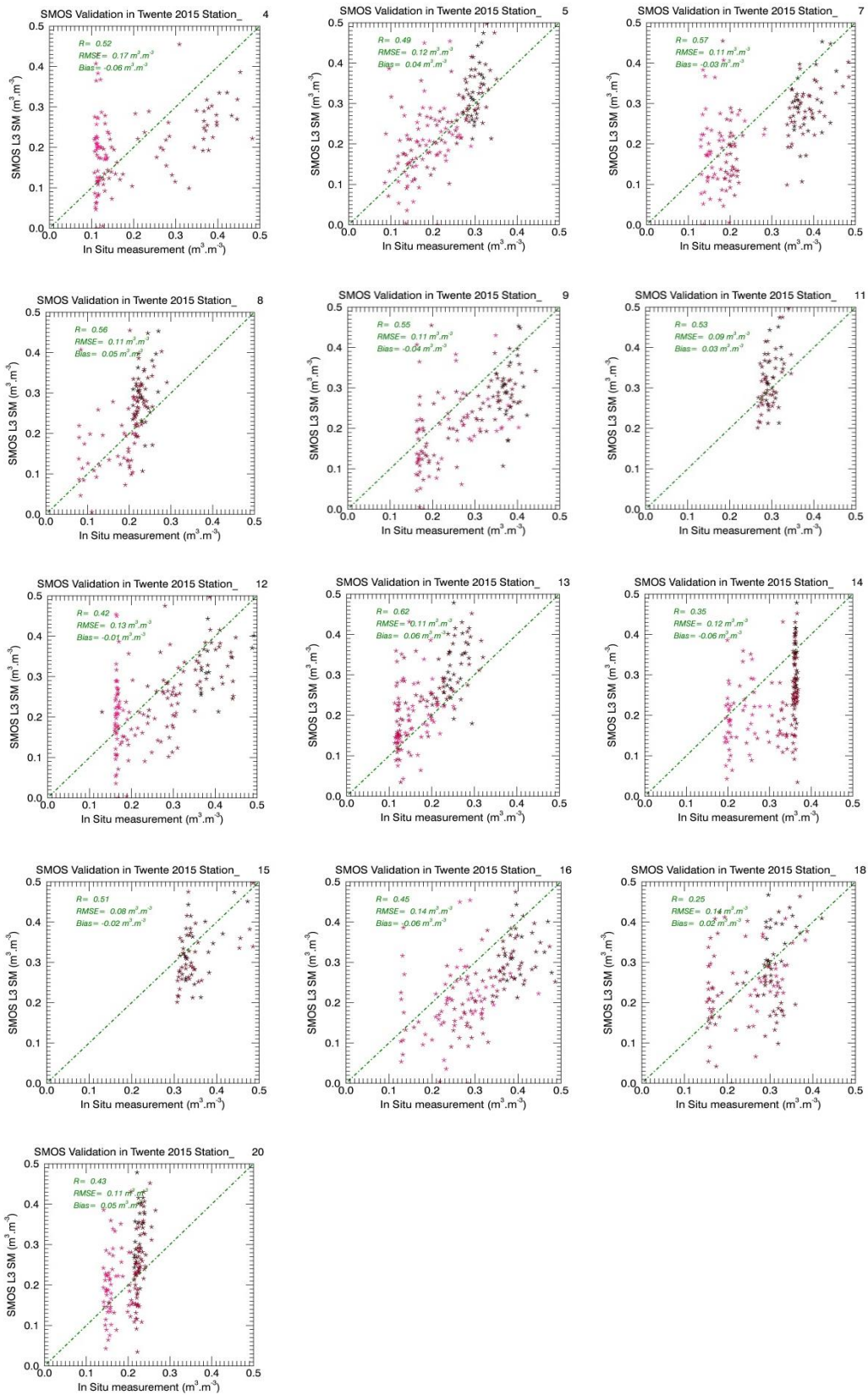


Figure 9 presents correlation between SMOS L3 SM and in situ data for individual stations in 2015.

### 6.2. Comparison of individual stations with SMAP L2 SM P

Original SMAP L2 SM P achieved from the ascending overpass is directly compared to soil moisture measurement at individual stations for years 2015 during period of the first of April till end of November. Statistical scores of comparison between the two data sets are presented in Table 8. Regarding to correlation, station 1 presents the highest correlation with value of 0.86 and lowest correlation is observed for station 14 with value of 0.32. On average, correlation value of 0.66 is monitored between the two datasets.

On average for all the stations, SMAP systematically represents wet biases during the period of study with value of 0.01 m<sup>3</sup>.m<sup>-3</sup> and the range of absolute values between 0 m<sup>3</sup>.m<sup>-3</sup> to 0.09 m<sup>3</sup>.m<sup>-3</sup> in station 1 and station 13, respectively. In terms of RMSD the highest value of 0.11 m<sup>3</sup>.m<sup>-3</sup> is monitored for stations 4, 8 13 and 20, while in station 3 the lowest value between the datasets is observed.

The correlation performances of the SMAP L2 SM P observation and particular station are demonstrated in Figure 10. Linear relationship and almost equal dynamic range of soil moisture for the both products in majority of stations are noticeable. However, at station 4 and 20 satellite based product shows higher range of dynamic range.

The Taylor diagram illustrating statistical results of comparison between SMOS and SMAP products respecting to individual in situ measurements for year 2015 are presented in Figure 11. In general, the diagram highlights higher correlation values for SMAP products compared to SMOS observation. Majority of correlation values for SMAP L2 SM P are observed between 0.55- 0.8, while for SMOS correlation value is monitored between 0.3- 0.6.

Table 8 statistical results of comparison between SMAP L2 SM P and individual stations form April till November 2015.

Station	R	RMSD (m <sup>3</sup> .m <sup>-3</sup> )	Bias (m <sup>3</sup> .m <sup>-3</sup> )
1	0.86	0.06	0
2	0.65	0.07	-0.04
3	0.64	0.05	-0.01
4	0.61	0.11	0.06
5	0.76	0.06	0.02
7	0.79	0.06	0.01
8	0.6	0.11	0.05
9	0.72	0.07	-0.04
12	0.51	0.08	0.03
13	0.81	0.11	0.09
14	0.32	0.1	-0.03
16	0.8	0.06	-0.03
18	0.69	0.07	-0.03
20	0.43	0.11	0.08
average	<b>0.66</b>	<b>0.08</b>	<b>0.01</b>

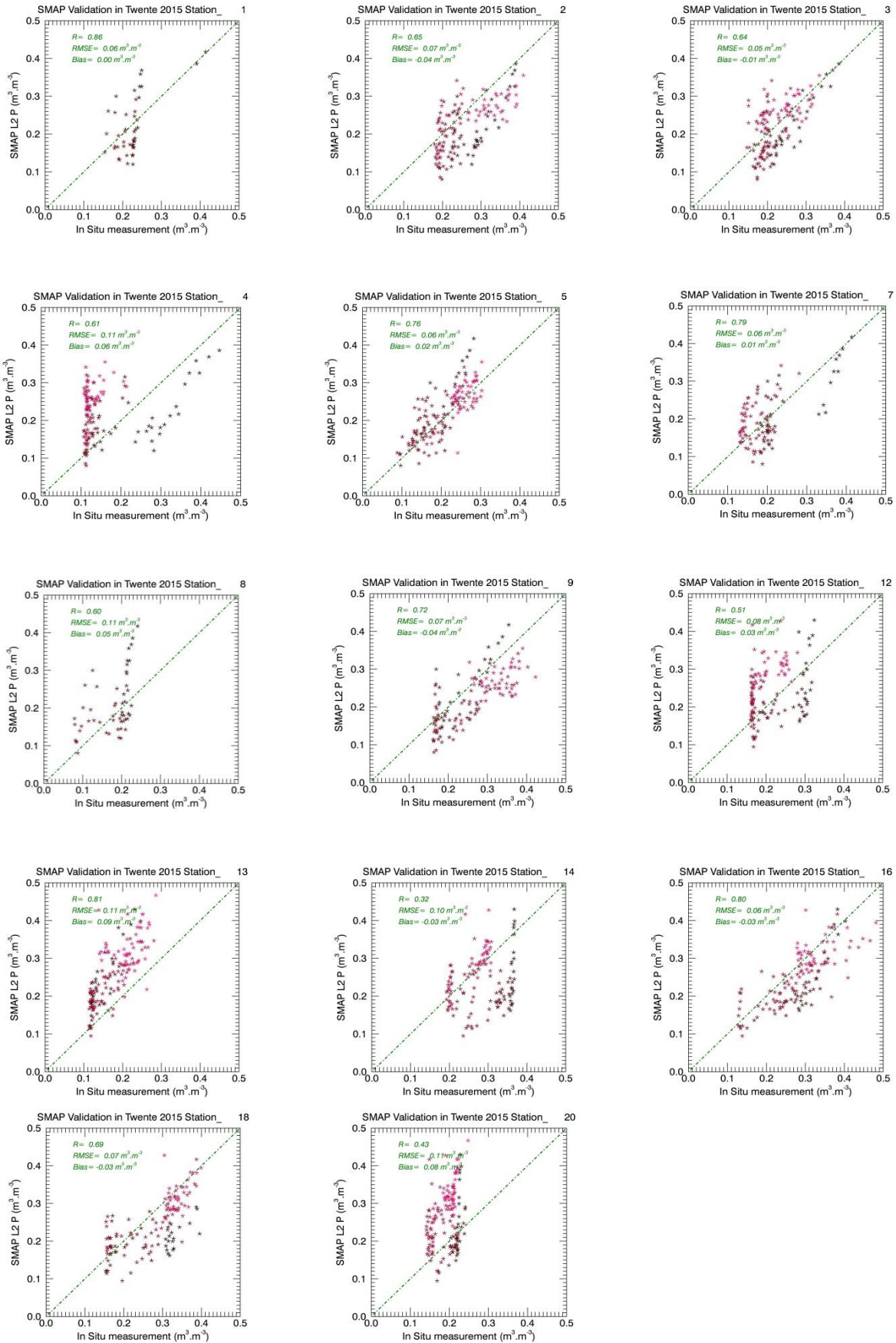


Figure 10, presents scatter plots between SMAP L2 SM P and individual stations from a period of first of April to November 31.

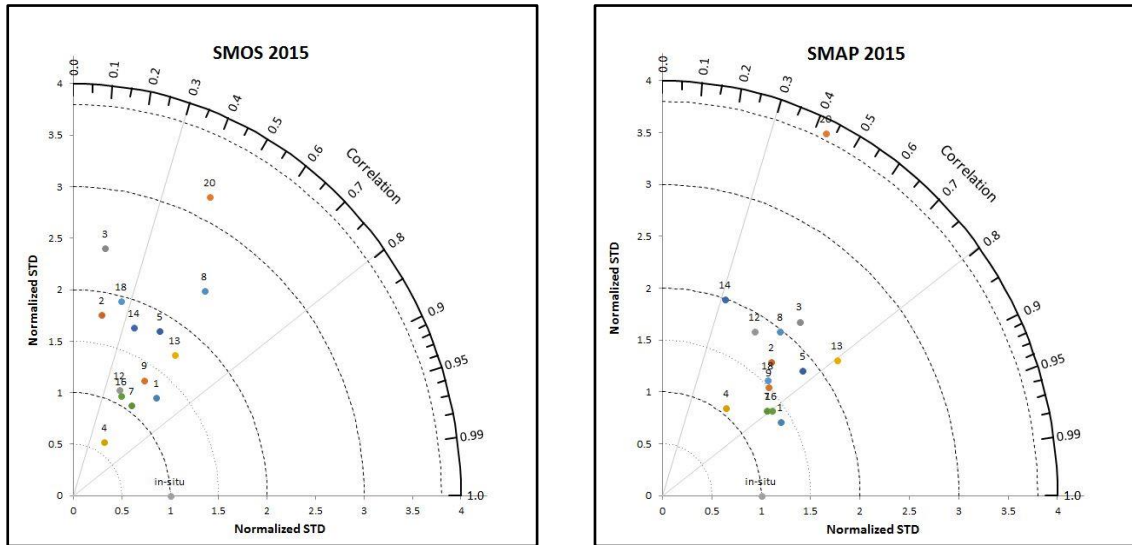


Figure 11 presents statistical scores of comparison between SMOS, SMAP and particular in situ measurements in 2015.

Almost all symbols are presenting above the line of normalized standard deviation 1, which indicates the variability of satellite-based soil moisture estimation in this period is higher than in situ measurements. Moreover, SMOS demonstrate larger dispersion in comparison with SMAP. Station 20 for both satellite observations presents very high standard deviation with low correlation value, which can be explained by the influence of dense vegetation cover on sensitivity of remotely sensed soil moisture estimation.

At station 4 larger soil moisture variation is found for SMAP compared to SMOS respect to reference dataset. During field experience station 4 was selected for visiting and lots of measurements were made. The observations indicated high value of soil moisture content in this station, while Probe measurements performance low values ( $0.1\text{m}^3\cdot\text{m}^{-3}$ ) without rainfall reaction. Consequently, it is arguable that, Probe measurements at station 4 do not represent the soil moisture content of the area in this specific time.

### 6.3. Comparison of upscaled in situ soil moisture with satellite observations

Time series of four surface soil moisture (SSM) products (*in-situ*, LHM and SMOS L3) for years 2012, 2013, 2014 and 2015 are compared in Figure 12. The *in-situ* measurements consist of spatially averaged of stations measurement ( $\bar{\theta}_{point}$ ) and domain estimation ( $\bar{\theta}_{Domain}^{point}$ ). In general,  $\bar{\theta}_{point}$  and  $\bar{\theta}_{Domain}^{point}$  have almost the same temporal variation and response to precipitation. However,  $\bar{\theta}_{Domain}^{point}$  is observed wetter than  $\bar{\theta}_{point}$ .

The SMOS observation and LHM simulated product follow the temporal dynamic of *in-situ* data. However, seasonal trend of the in-situ measurements is reproduced better with LHM product, particularly in the year 2012, when the SMOS observation was highly distributed by Radio frequency interference (RFI). Moreover, the three products have an agreement in detection of precipitation event, although reaction of SMOS observation is much higher than LHM product and in situ measurement, which can be described with water ponding effects when soil is saturated during intensive rainfall (Al-Yaari et al., 2014; Jackson et al., 2012).

During cold period of the year 2012, an abrupt drop in soil moisture measurements and very low values for SMOS observation (near zero) are monitored. The steep decrease in measured and observed soil moisture values can be explained by soil freezing. However, in the most the freezing period SMOS observation was flagged and the data is excluded. The LHM product does not influence by soil freezing effect, which can be described by the depth of simulation.

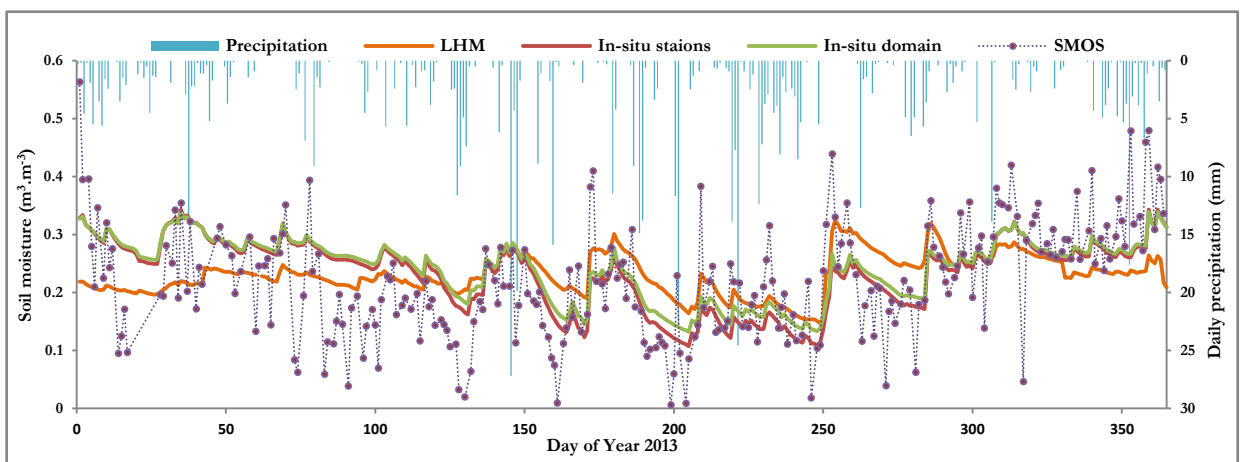
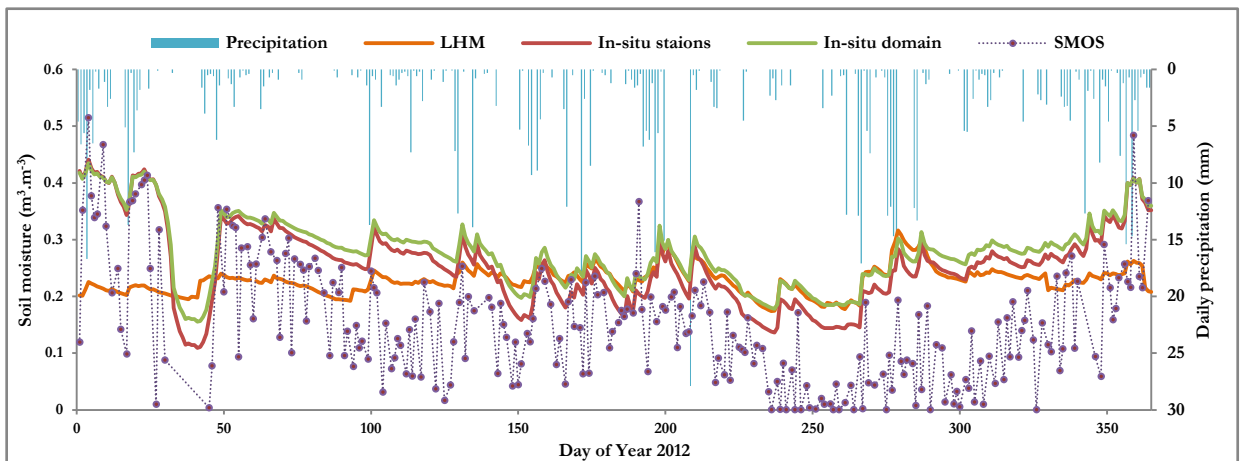
Generally, the SMOS series illustrates larger dynamic range than in-situ and simulated product. The  $\bar{\theta}_{Domain}^{point}$  have mean values of 0.279 m<sup>3</sup>.m<sup>-3</sup>, 0.243 m<sup>3</sup>.m<sup>-3</sup>, 0.303 m<sup>3</sup>.m<sup>-3</sup> and 0.299 m<sup>3</sup>.m<sup>-3</sup> with standard deviation of 0.061 m<sup>3</sup>.m<sup>-3</sup>, 0.053 m<sup>3</sup>.m<sup>-3</sup>, 0.043 m<sup>3</sup>.m<sup>-3</sup> and 0.067 m<sup>3</sup>.m<sup>-3</sup> in years 2012, 2013, 2014 and 2015, respectively. While, for SMOS L3 mean values of 0.153 m<sup>3</sup>.m<sup>-3</sup>, 0.219 m<sup>3</sup>.m<sup>-3</sup>, 0.258 m<sup>3</sup>.m<sup>-3</sup> and 0.252 m<sup>3</sup>.m<sup>-3</sup>.with standard deviation of 0.105 m<sup>3</sup>.m<sup>-3</sup>, 0.097 m<sup>3</sup>.m<sup>-3</sup>, 0.083 m<sup>3</sup>.m<sup>-3</sup> and 0.113 m<sup>3</sup>.m<sup>-3</sup>.are observed for the consecutive years.

The up-scaling strategy does not influence correlation between satellite-based observation and the in-situ measurements. The same correlation values among  $\bar{\theta}_{point}$ ,  $\bar{\theta}_{Domain}^{point}$  and the SMOS product with values of 0.66, 0.57, 0.6 and 0.55 are observed. However, dry biases between the SMOS observation and  $\bar{\theta}_{Domain}^{point}$  are found higher than  $\bar{\theta}_{point}$  with average values of -0.063 m<sup>3</sup>.m<sup>-3</sup> and -0.035 m<sup>3</sup>.m<sup>-3</sup>, respectively.

The scatter plots presenting the correlation performances between SMOS observation and *in-situ* measurements ( $\bar{\theta}_{point}$  and  $\bar{\theta}_{Domain}^{point}$ ) for years 2012, 2013, 2014 and 2015 are displayed in Figure 13 and Figure 14, respectively. The scatter plots underline higher range of observed soil moisture and negative biases for SMOS product spatially in the year 2012. Statistical scores of comparison between SMOS and *in-situ* measurements are presented in Table 9.

Table 9 presents statistics of comparison among *in-situ* measurements (average of station and upscaled), SMOS and SMAP observations for years 2012, 2013, 2014 and 2015.

		SMOS-in situ	SMOS-in situ	SMAP-in situ	SMAP-in situ
		Domain	Stations	Domain	Stations
2012	RMSD	0.15	0.13		
	MAE	0.13	0.11		
	R	0.66	0.66		
	bias	-0.13	-0.1		
2013	RMSD	0.08	0.08		
	MAE	0.06	0.06		
	R	0.57	0.57		
	bias	-0.02	-0.01		
2014	RMSD	0.08	0.07		
	MAE	0.07	0.05		
	R	0.60	0.60		
	bias	-0.05	-0.02		
2015	RMSD	0.1	0.1	0.06	0.06
	MAE	0.08	0.07	0.05	0.04
	R	0.55	0.55	0.82	0.82
	bias	-0.05	-0.01	-0.05	-0.02



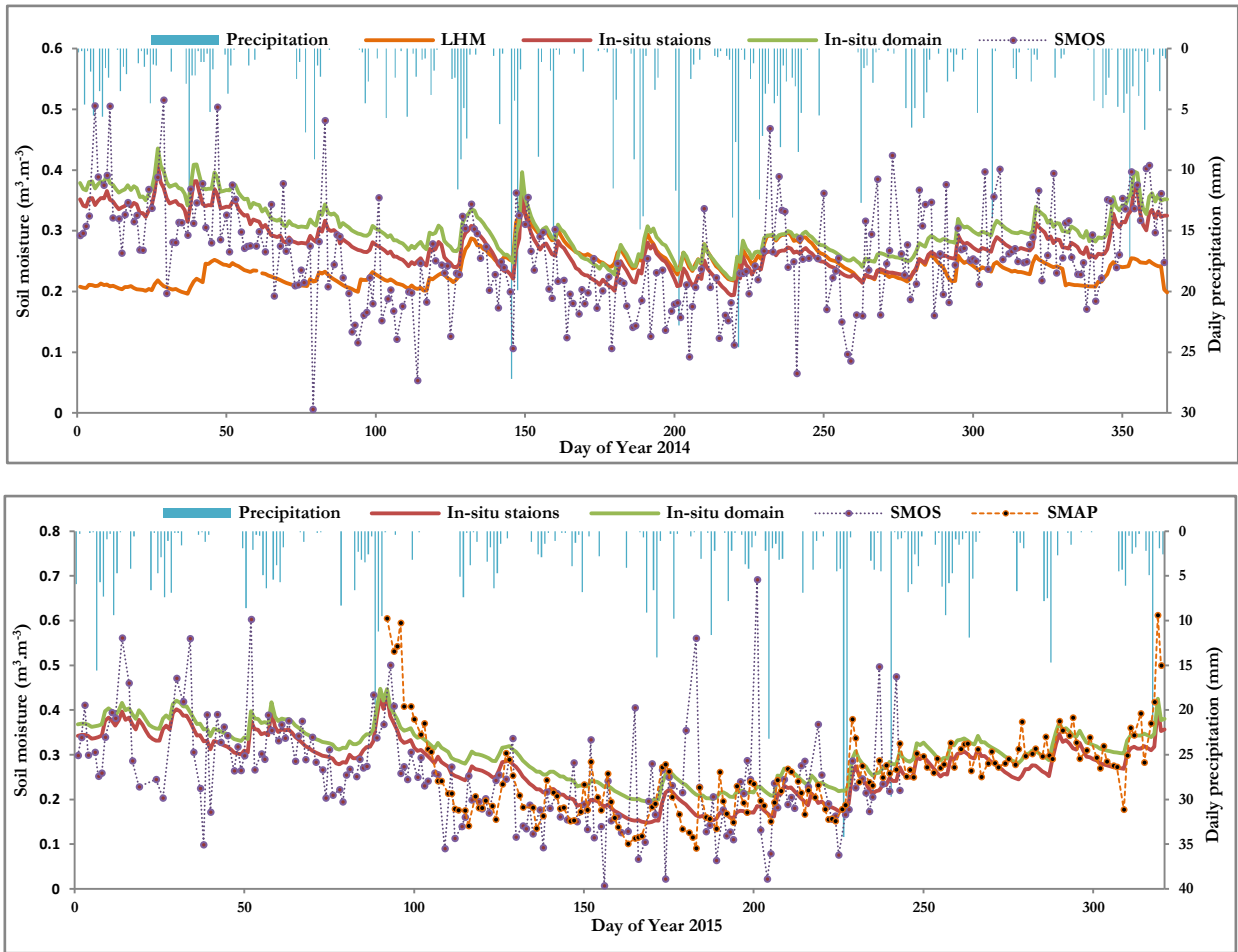
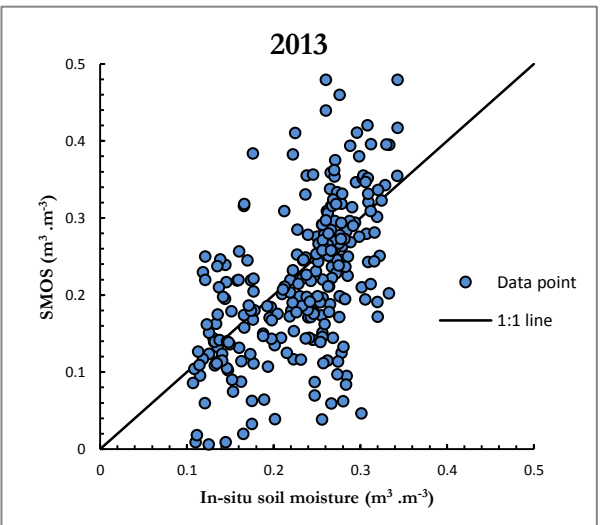
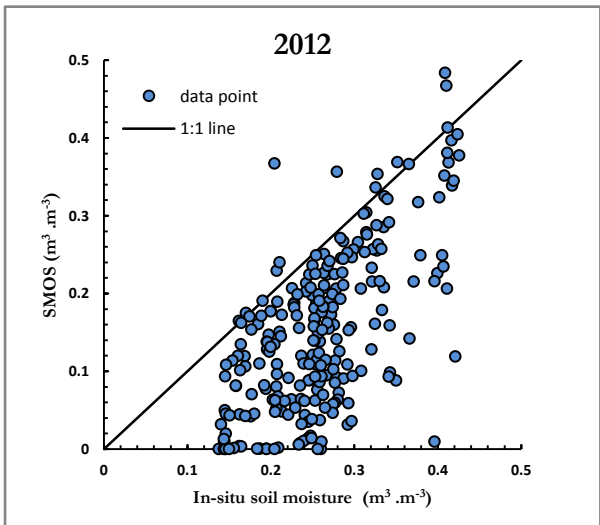


Figure 12 soil moisture evaluation of in-situ measurements (average of station and upscaled) LHM product and SMOS and SMAP observation along with daily rainfall in Twente region.



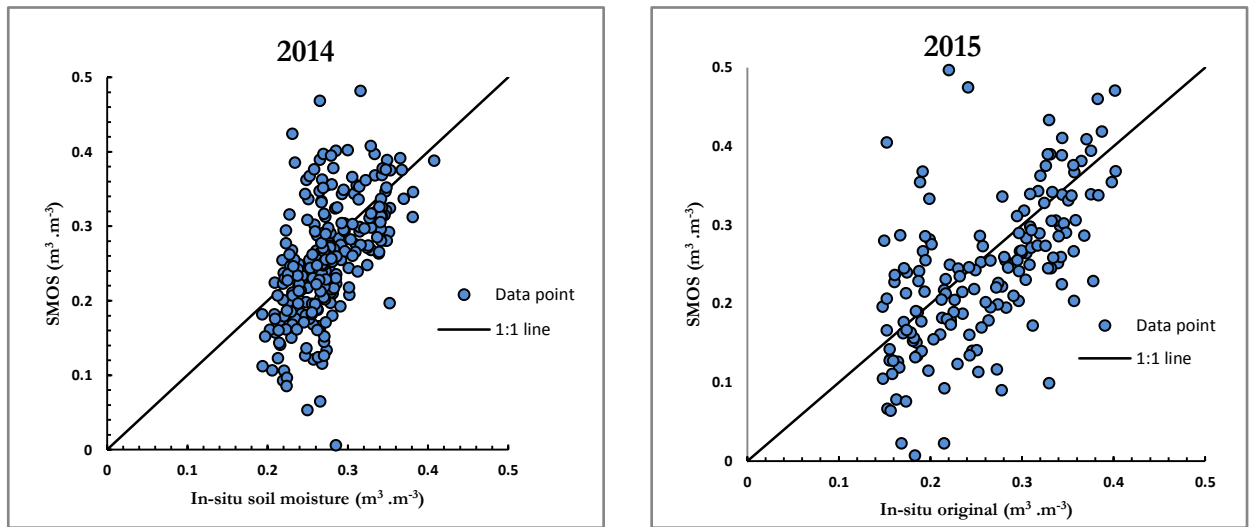


Figure 13 demonstrates results of comparison between mean in-situ measurement  $\bar{\theta}_{point}$  and SMOS observation for years 2012, 2013, 2014 and 2015

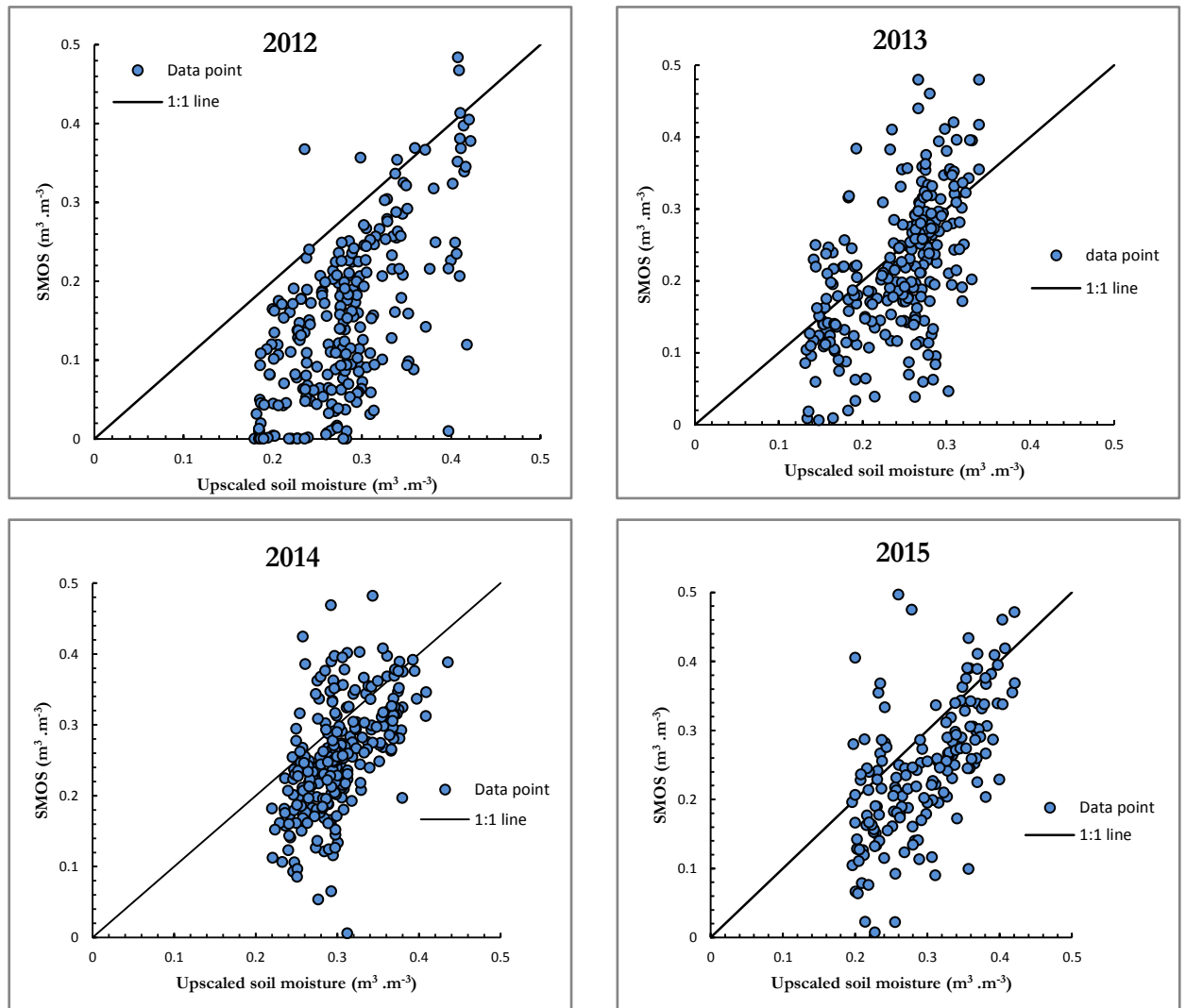


Figure 14 demonstrates results of comparison between mean in-situ measurement  $\bar{\theta}_{Domain}^{point}$  and SMOS observation for years 2012, 2013, 2014 and 2015.

The performance of two *in-situ* measurements ( $\bar{\theta}_{point}$  and  $\bar{\theta}_{Domain}^{point}$ ) soil moisture in comparison to satellite-based observation (SMAP) for period of April 1<sup>st</sup> till November 16<sup>th</sup> in the year 2015 are presented in Figure 15. In general, the temporal dynamics of *in-situ* measurements monitored by stations and SMAP observation are found quit similar. For example in Julian day 317 with extensive rainfall *in-situ* and SMAP product present sharp increases in soil moisture value. However, dry biases in the mean and the soil moisture change in response to rainfall can be remarked. A probable reason for negative biases of SMOS and SMAP products can be associated with very high sand content at the station locations. Recently, González-Zamora et al., 2015 discussed that soil with high sand content preformed drier condition than soil with finer texture. Since all the stations are located on sandy and loamy sandy soil, dry biases that found for the both satellite based observation can be rational.

The correlation performances between *in-situ* measurements ( $\bar{\theta}_{point}$  and  $\bar{\theta}_{Domain}^{point}$ ) and SMAP observation are presented in Figure 15. The comparison of *in-situ* measurements with SMAP observation showed an agreements with correlation value of 0.82 for the both  $\bar{\theta}_{point}$  and  $\bar{\theta}_{Domain}^{point}$ , while higher dry biases between SMAP and up-scaled *in-situ* measurements can be noted. Statistical scores of comparison between SMAP and in-situ measurements ( $\bar{\theta}_{point}$  and  $\bar{\theta}_{Domain}^{point}$ ) are presented in Table 9.

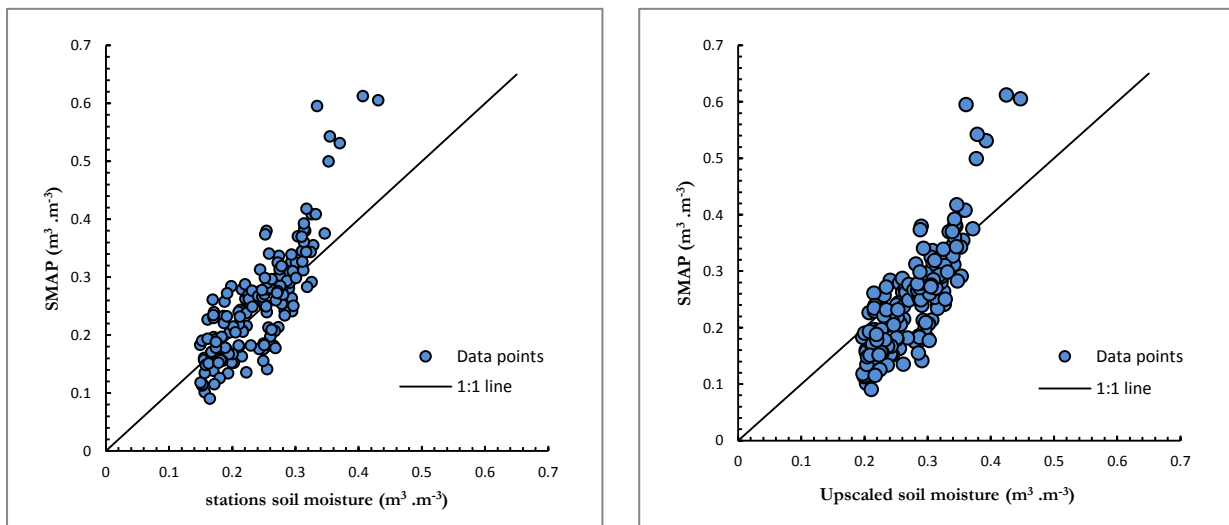


Figure 15 illustrates scatter plots between mean in-situ measurement ( $\bar{\theta}_{point}$ ), upscaled in-situ measurement ( $\bar{\theta}_{Domain}^{point}$ ) and SMAP observation.

## 7.FINAL REMARKS

### 7.1. Conclusion

Since satellite-based surface soil moisture observations might disturb by numerous factors such as vegetation covers, surface roughness, soil freezing, extensive rainfall, assessment of the accuracy and reliability of these data science products before using them is crucial. *In-situ* measurements can be employed as a reference dataset to compare either spatially distributed soil moisture simulated products or remotely sensed observations to estimates errors and biases of the distributed products. The results of evaluation can be utilized for improving retrieval algorithms or just for awareness of potential users.

The validation activity that conducted in this research used *in-situ* surface soil moisture data collected by 20 monitoring stations located in Twente region to assess the reliability of LHM, SMOS L3 and SMAP L2 P products. First the reliability of the each spatially distributed product is evaluated by measurement obtained from individual station. Then LHM product is employed to derive and develop up-scaling functions for transferring averaged point measurements to domain scale. Finally, *in-situ* up-scaled soil moisture measurements are used to evaluate the satellite-based observations.

In general, the results demonstrate that LHM simulated product captures temporal dynamic of surface soil moisture collected by individual station for summer period. However, the product is not able to reproduce surface soil moisture in wet seasons, which probably is because of the inability of model to properly simulate the interaction between the vadose zone and groundwater. On average, for the summer period, correlation value of 0.67 with positive biases of  $0.02\text{m}^3.\text{m}^{-3}$  and RMSD equal to  $0.1\text{m}^3.\text{m}^{-3}$  are found for the LHM product.

The SMOS soil moisture product follows temporal dynamic of referenced soil moisture. However, the correlation between datasets is highly dependent on RFI. In the year 2011 with high RFI probability, SMOS correlation respect to the individual station and mean correlation value presents the worst result compared to following years. Continuous dry biases are found for SMOS product from the year 2010 to 2015, which probably can be either the result of low level of RFI or high sand content at the area.

The SMAP product captures the temporal variability of measurements collected by the monitoring stations, even though *in-situ* do not measure the same quantity of coarse resolution satellite-based product. Correlation values of 0.82 were obtained between the SMAP product and *in-situ* measurement for the averaged individual station and the study domain. Negative bias of  $-0.05\text{m}^3.\text{m}^{-3}$  is also monitored for the SMAP. However, The SMAP fulfils the accuracy requirement by the satellite mission with centred root mean squared of  $0.04\text{m}^3.\text{m}^{-3}$ .

Up-scaled mean soil moisture measurements is found slightly wetter than mean soil moisture measured by individual stations. Since the three spatially distributed products demonstrate dry biases, the up-scaling strategy increases the biases in mean values of spatially distributed products and in-situ datasets. However, RMSD and correlation between the datasets are not influenced by up-scaling process.

## **7.2. Recommendation**

Further analysis for the products in the study area might include:

- Decomposition of uncertainty between LHM fine resolutions spatially distributed soil moisture simulated product and coarse scale SMOS and SMAP retrieval soil moisture.
- Since LHM is not able to properly reproduce temporal variability of soil moisture for wet seasons, the problem can be considered for future research.
- Temporal stability analysis can be employed as an alternative up-scaling tool for more detailed validation of remotely sensed soil moisture products.

## LIST OF REFERENCES

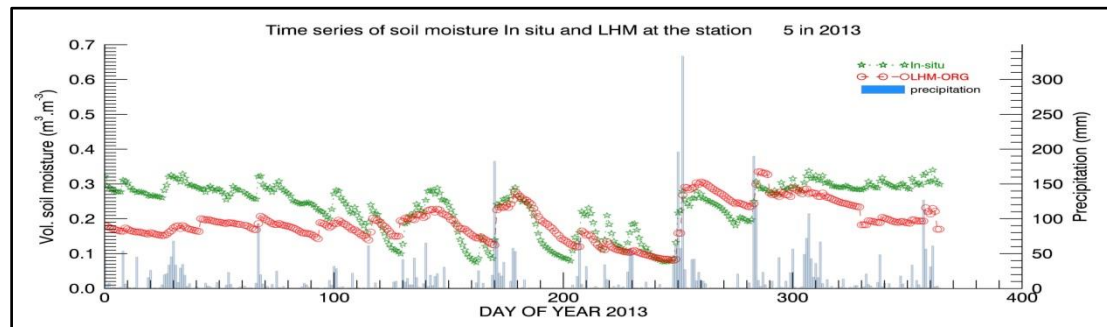
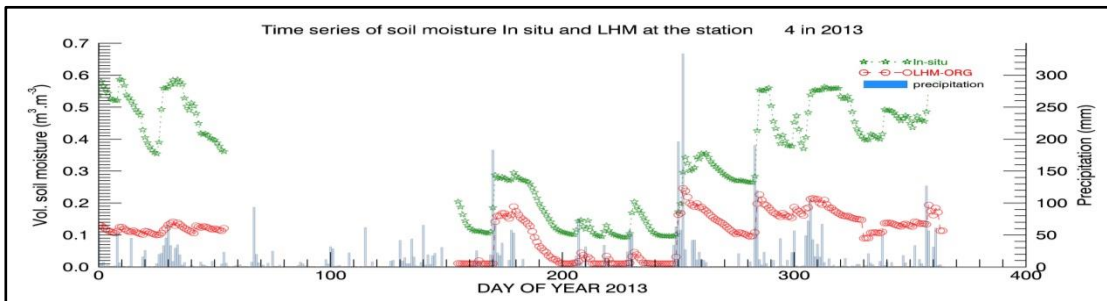
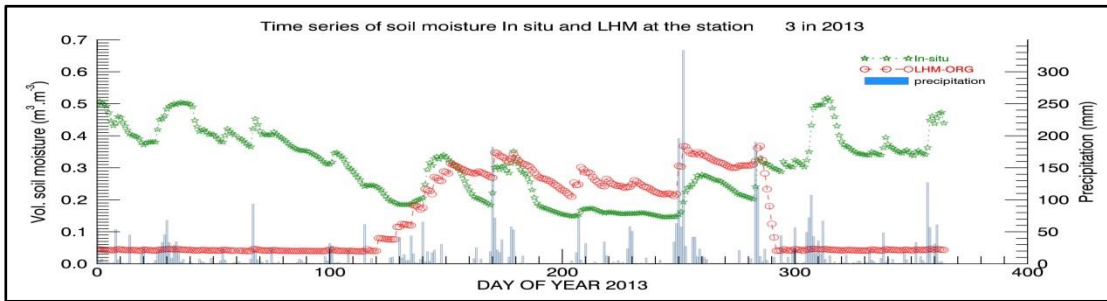
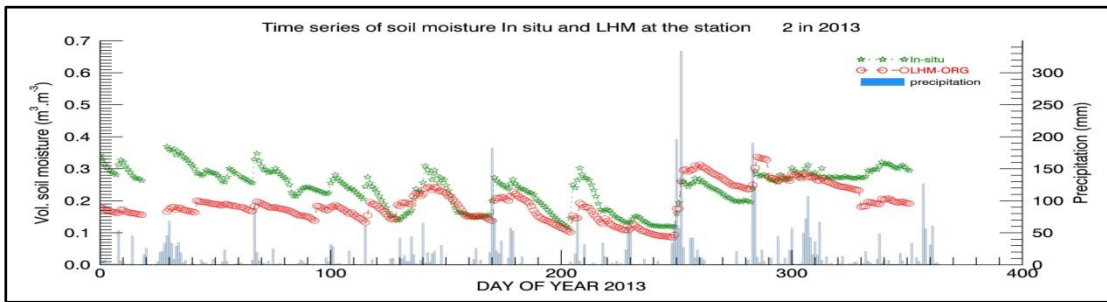
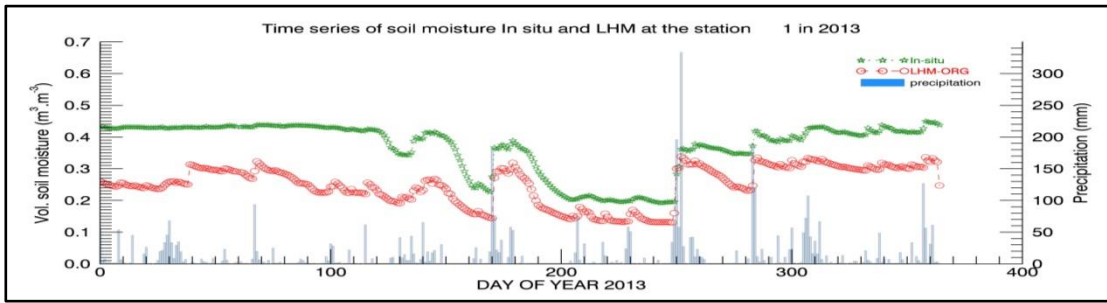
---

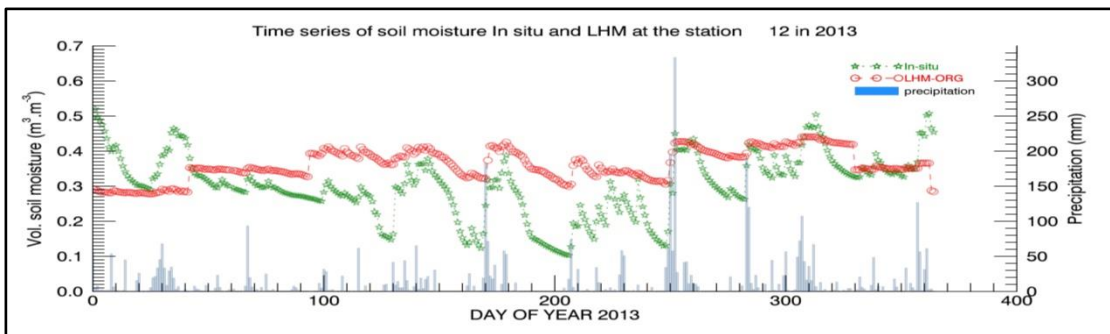
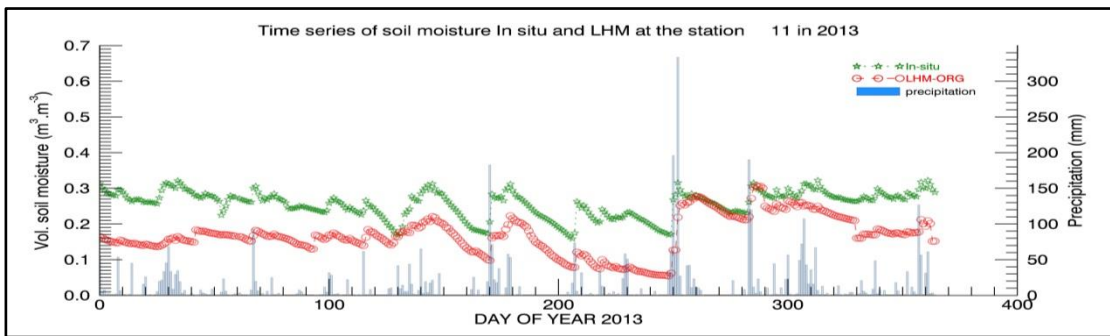
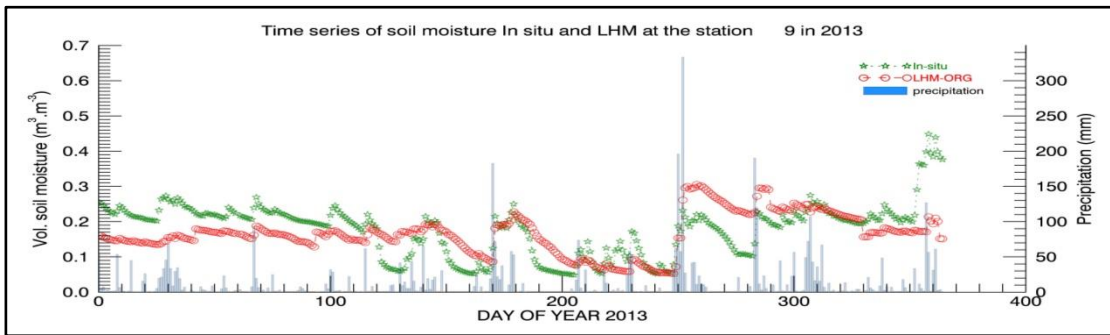
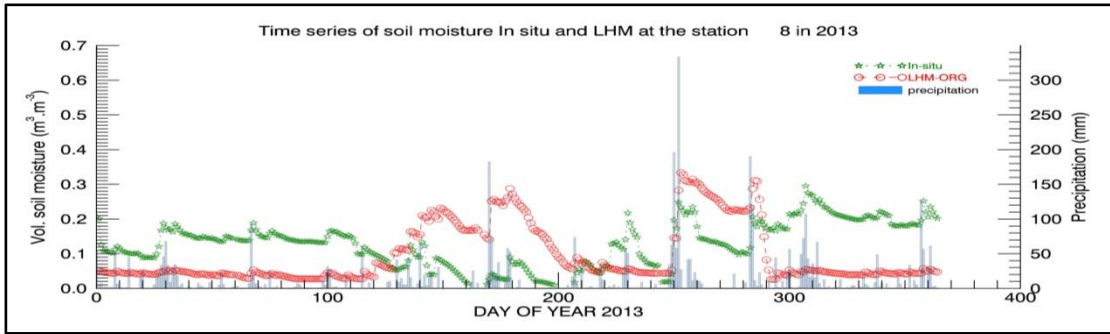
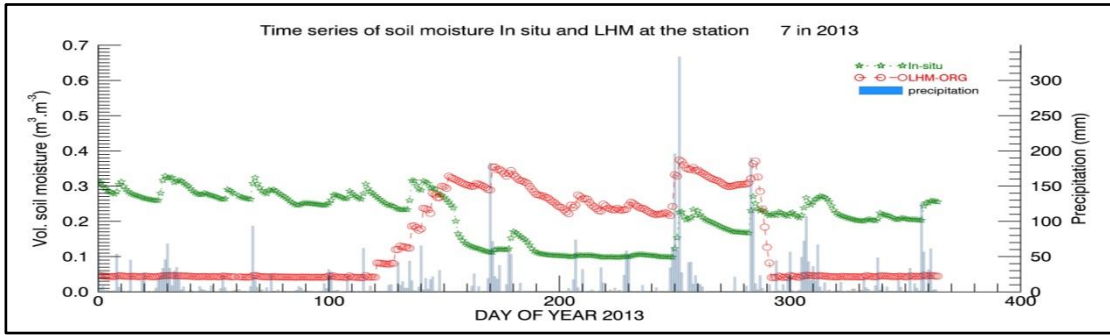
- Albergel, C., de Rosnay, P., Gruhier, C., Muñoz-Sabater, J., Hasenauer, S., Isaksen, L., ... Wagner, W. (2012). Evaluation of remotely sensed and modelled soil moisture products using global ground-based in situ observations. *Remote Sensing of Environment*, 118, 215–226. doi:10.1016/j.rse.2011.11.017
- Al-Yaari, a., Wigneron, J. P., Ducharne, a., Kerr, Y., de Rosnay, P., de Jeu, R., ... Mialon, a. (2014). Global-scale evaluation of two satellite-based passive microwave soil moisture datasets (SMOS and AMSR-E) with respect to Land Data Assimilation System estimates. *Remote Sensing of Environment*, 149, 181–195. doi:10.1016/j.rse.2014.04.006
- Bircher, S., Skou, N., Jensen, K. H., Walker, J. P., & Rasmussen, L. (2012). A soil moisture and temperature network for SMOS validation in Western Denmark. *Hydrology and Earth System Sciences*, 16(5), 1445–1463. doi:10.5194/hess-16-1445-2012
- Bitar, A. Al, Leroux, D., Kerr, Y. H., Member, S., Merlin, O., Richaume, P., ... Wood, E. F. (2012). Evaluation of SMOS Soil Moisture Products Over Continental U . S . Using the SCAN / SNOTEL Network. *IEEE Transactions on Geoscience and Remote Sensing*, 50(5), 1572–1586.
- Brocca, L., Hasenauer, S., Lacava, T., Melone, F., Moramarco, T., Wagner, W., ... Bittelli, M. (2011). Soil moisture estimation through ASCAT and AMSR-E sensors: An intercomparison and validation study across Europe. *Remote Sensing of Environment*, 115(12), 3390–3408. doi:10.1016/j.rse.2011.08.003
- Brocca, L., Melone, F., Moramarco, T., Wagner, W., & Hasenauer, S. (2010). ASCAT soil wetness index validation through in situ and modeled soil moisture data in central Italy. *Remote Sensing of Environment*, 114(11), 2745–2755. doi:10.1016/j.rse.2010.06.009
- Crow, W. T., Berg, A. a, Cosh, M. H., Loew, A., Mohanty, B. P., Panciera, R., ... Walker, J. P. (2012). Upscaling Sparse Ground-Based Soil Moisture Observations for the Validation of Coarse-Resolution Satellite Soil Moisture Products, (2011), 1–20. doi:10.1029/2011RG000372.1.INTRODUCTION
- Crow, W. T., Ryu, D., & Famiglietti, J. S. (2005). Upscaling of field-scale soil moisture measurements using distributed land surface modeling. *Advances in Water Resources*, 28(1), 1–14. doi:10.1016/j.advwatres.2004.10.004
- Das, N. N., Entekhabi, D., & Njoku, E. G. (2011). An algorithm for merging SMAP radiometer and radar data for high-resolution soil-moisture retrieval. *IEEE Transactions on Geoscience and Remote Sensing*, 49(5), 1504–1512. doi:10.1109/TGRS.2010.2089526
- De Lange, W. J., Prinsen, G. F., Hoogewoud, J. C., Veldhuizen, A. A., Verkaik, J., Oude Essink, G. H. P., ... Kroon, T. (2014). An operational, multi-scale, multi-model system for consensus-based, integrated water management and policy analysis: The Netherlands Hydrological Instrument. *Environmental Modelling & Software*, 59, 98–108. doi:10.1016/j.envsoft.2014.05.009
- Delsman, J. R., Veldhuizen, A. a., & Snepvangers, J. (2008). *Netherlands Hydrological Modeling Instrument. Proc. of Modflow and More: Ground Water and Public Policy*. Retrieved from [http://www.nhi.nu/documenten/Modflowandmore\\_Netherlands\\_hydrological\\_modeling\\_instrument.pdf](http://www.nhi.nu/documenten/Modflowandmore_Netherlands_hydrological_modeling_instrument.pdf)
- Dente, L., Su, Z., & Wen, J. (2012). Validation of SMOS soil moisture products over the Maqu and Twente Regions. *Sensors (Switzerland)*, 12(8), 9965–9986. doi:10.3390/s120809965
- Dente, L., Vekerdy, Z., Su, B., & Ucer, M. (2011). *Soil Moisture and Soil Temperature Monitoring Network*.
- Du, J. (2012). A method to improve satellite soil moisture retrievals based on Fourier analysis. *Geophysical Research Letters*, 39(15), 1–4. doi:10.1029/2012GL052435
- Entekhabi, D., Yueh, S., O'Neill, P. E., Kellogg, K., Allen, A., & Bindlish, R. (2014). *SMAP Handbook*.

- Gherboudj, I., Magagi, R., Goïta, K., Berg, A. a., Toth, B., & Walker, A. (2012). Validation of SMOS data over agricultural and boreal forest areas in Canada. *IEEE Transactions on Geoscience and Remote Sensing*, 50(5 PART 1), 1623–1635. doi:10.1109/TGRS.2012.2188532
- González-Zamora, Á., Sánchez, N., Martínez-Fernández, J., Gumuzzio, Á., Piles, M., & Olmedo, E. (2015). Long-term SMOS soil moisture products: A comprehensive evaluation across scales and methods in the Duero Basin (Spain). *Physics and Chemistry of the Earth, Parts A/B/C*. doi:10.1016/j.pce.2015.05.009
- Heathman, G. C., Cosh, M. H., Han, E., Jackson, T. J., McKee, L., & McAfee, S. (2012). Field scale spatiotemporal analysis of surface soil moisture for evaluating point-scale in situ networks. *Geoderma*, 170, 195–205. doi:10.1016/j.geoderma.2011.11.004
- Houser, P. R., De lannoy, G., & Walker, J. P. (2010). *Assimilation, Data*. (W. Lahoz, B. Khattatov, & R. Menard, Eds.). The Netherlands: Springer.
- Jackson, T. J., Bindlish, R., Cosh, M. H., Zhao, T., Starks, P. J., Bosch, D. D., ... Leroux, D. (2012). Validation of soil moisture and Ocean Salinity (SMOS) soil moisture over watershed networks in the U.S. *IEEE Transactions on Geoscience and Remote Sensing*, 50(5 PART 1), 1530–1543. doi:10.1109/TGRS.2011.2168533
- Kerr, Y. H., Berthon, L., Mialon, A., Cabot, F., Al Bitar, A., Richaume, P., ... Jacqueline, E. (2014). CATDS LEVEL 3 - Data product description - Soil Moisture and Brightness Temperature, (3.a).
- Kerr, Y. H., Jacqueline, E., Al Bitar, A., Cabot, F., Mialon, A., & Richaume, P. (2013). *CATDS SMOS L3 soil moisture retrieval processor, Algorithm Theoretical Baseline Document (ATBD)*.
- Kerr, Y. H., Waldteufel, P., Richaume, P., Wigneron, J. P., Ferrazzoli, P., Mahmoodi, A., ... Delwart, S. (2012). The SMOS Soil Moisture Retrieval Algorithm. *Geoscience and Remote Sensing*, 50(5), 1384–1403.
- Kerr, Y. H., Waldteufel, P., Wigneron, J. P., Martinuzzi, J. M., Font, J., & Berger, M. (2001). Soil moisture retrieval from space: The Soil Moisture and Ocean Salinity (SMOS) mission. *IEEE Transactions on Geoscience and Remote Sensing*, 39(8), 1729–1735. doi:10.1109/36.942551
- Kornelsen, K. C., & Coulibaly, P. (2015). Reducing multiplicative bias of satellite soil moisture retrievals. *Remote Sensing of Environment*, 165, 109–122. doi:10.1016/j.rse.2015.04.031
- Miernecki, M., Wigneron, J., Lopez-baeza, E., Kerr, Y., Jeu, R. De, Lannoy, G. J. M. De, ... Richaume, P. (2014). Comparison of SMOS and SMAP soil moisture retrieval approaches using tower-based radiometer data over a vineyard field. *Remote Sensing of Environment*, 154, 89–101. doi:10.1016/j.rse.2014.08.002
- O'Neill, P., Njoku, E. G., & Jackson, T. (2015). *the SMAP Algorithm Theoretical Basis Document L2 & L3 soil moisture (Passive) data products*.
- Panciera, R., Walker, J. P., Jackson, T. J., Gray, D. a., Tanase, M. a., Ryu, D., ... Hacker, J. M. (2014). The soil moisture active passive experiments (SMAPEX): Toward soil moisture retrieval from the SMAP mission. *IEEE Transactions on Geoscience and Remote Sensing*, 52(1), 490–507. doi:10.1109/TGRS.2013.2241774
- Petropoulos, G. P., Ireland, G., & Barrett, B. (2015). Surface soil moisture retrievals from remote sensing: Current status, products & future trends. *Physics and Chemistry of the Earth, Parts A/B/C*. doi:10.1016/j.pce.2015.02.009
- Qin, J., Zhao, L., Chen, Y., Yang, K., Yang, Y., Chen, Z., & Lu, H. (2015). Inter-comparison of spatial upscaling methods for evaluation of satellite-based soil moisture. *Journal of Hydrology*, 523, 170–178. doi:10.1016/j.jhydrol.2015.01.061
- Qiu, J., Mo, X., Liu, S., Lin, Z., Yang, L., Song, X., ... Wagner, W. (2013). Intercomparison of microwave remote-sensing soil moisture data sets based on distributed eco-hydrological model simulation and in situ measurements over the North China Plain. *International Journal of Remote Sensing*, 34(19), 6587–6610. doi:10.1080/01431161.2013.788799
- Rötzer, K., Montzka, C., Bogen, H., Wagner, W., Kerr, Y. H., Kidd, R., & Vereecken, H. (2014).

- Catchment scale validation of SMOS and ASCAT soil moisture products using hydrological modeling and temporal stability analysis. *Journal of Hydrology*, 519, 934–946. doi:10.1016/j.jhydrol.2014.07.065
- Sabaghy, S. (2013). *Soil moisture retrieval from combined Active / Passive Microwave Observations over the Regge and Dinkel* Soil moisture retrieval from combined Active / Passive Microwave Observations over the Regge and Dinkel.
- Sánchez, N., Martínez-Fernánadez, J., Scaini, A., & Pérez-Gutierrez, C. (2012). Validation of the SMOS L2 soil moisture data in the REMEDHUS network (Spain). *IEEE Transactions on Geoscience and Remote Sensing*, 50(5 PART 1), 1602–1611. doi:10.1109/TGRS.2012.2186971
- Su, C., Ryu, D., Crow, W. T., & Western, A. W. (2014). Stand-alone error characterisation of microwave satellite soil moisture using a Fourier method. *Remote Sensing of Environment*, 154, 115–126. doi:10.1016/j.rse.2014.08.014
- Taylor, K. E. (2001). in a Single Diagram. *Journal of Geophysical Research*, 106(D7), 7183–7192. doi:10.1029/2000JD900719
- Tuttle, S. E., & Salvucci, G. D. (2014). A new approach for validating satellite estimates of soil moisture using large-scale precipitation: Comparing AMSR-E products. *Remote Sensing of Environment*, 142, 207–222. doi:10.1016/j.rse.2013.12.002
- van Walsum, P. E. V., Veldhuizen, A. A., & Groenendijk, P. (2014). *Simgro 7.2.25 Theory and model implementation*.
- van Walsum, P. E. V. (2015). *Simgro v7.2.27 Input out put refrence manual*.
- Western, A. W., Grayson, R. B., & Blöschl, G. (2002). SCALING OF SOIL MOISTURE: A Hydrologic Perspective. *Annual Review of Earth and Planetary Sciences*, 30(1), 149–180. doi:10.1146/annurev.earth.30.091201.140434
- Xia, Y., Sheffield, J., Ek, M. B., Dong, J., Chaney, N., Wei, H., ... Wood, E. F. (2014). Evaluation of multi-model simulated soil moisture in NLDAS-2. *Journal of Hydrology*, 512, 107–125. doi:10.1016/j.jhydrol.2014.02.027
- Zeng, J., Li, Z., Chen, Q., & Bi, H. (2014). A simplified physically-based algorithm for surface soil moisture retrieval using AMSR-E data. *Frontiers of Earth Science*, 8(3), 427–438. doi:10.1007/s11707-014-0412-4
- Zeng, J., Li, Z., Chen, Q., Bi, H., Qiu, J., & Zou, P. (2015). Evaluation of remotely sensed and reanalysis soil moisture products over the Tibetan Plateau using in-situ observations. *Remote Sensing of Environment*, 163, 91–110. doi:10.1016/j.rse.2015.03.008

# APPENDIX





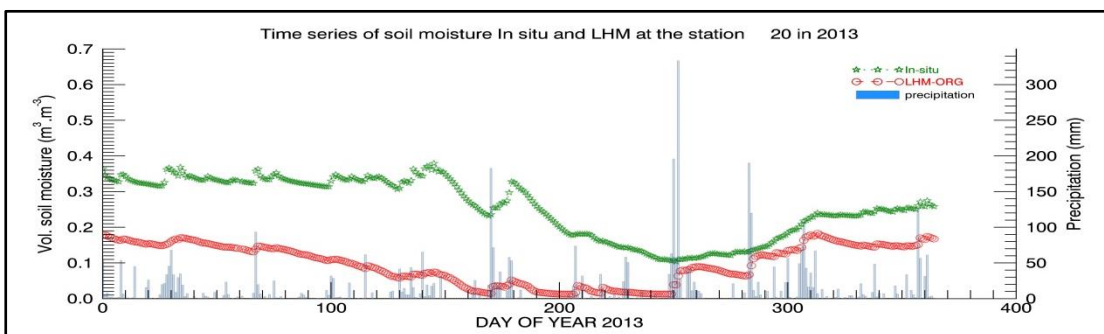
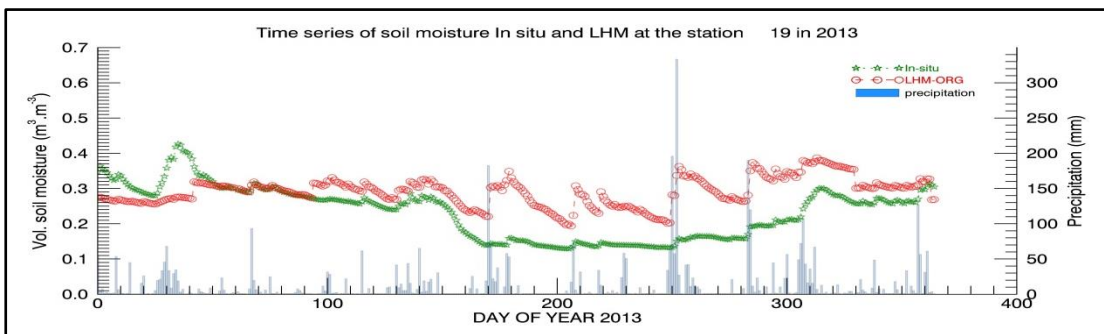
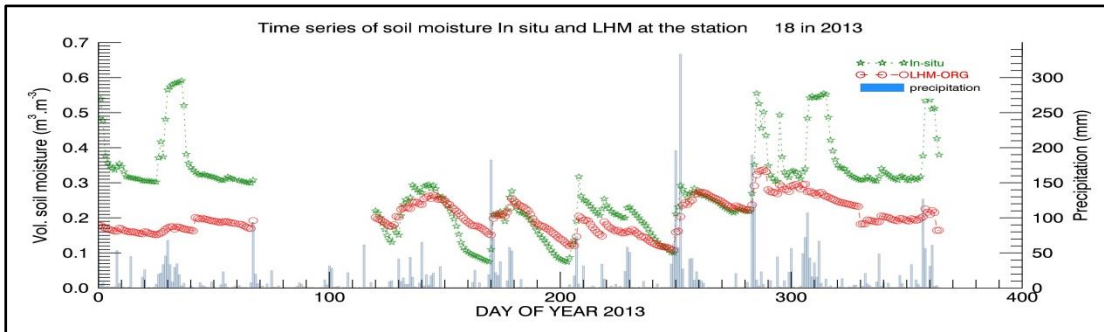
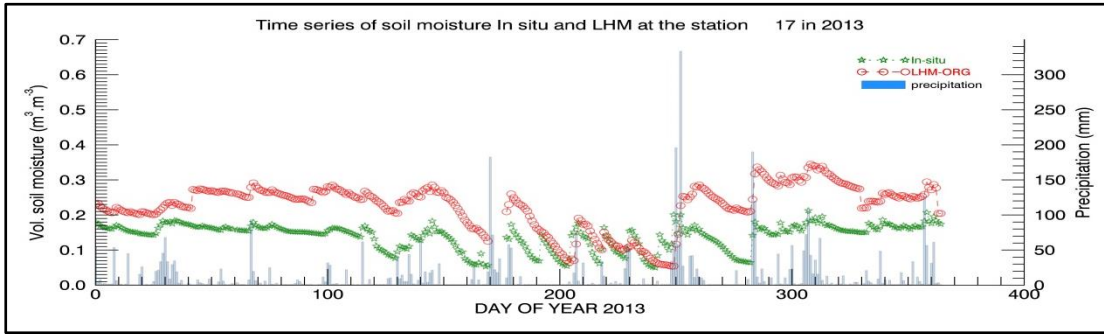
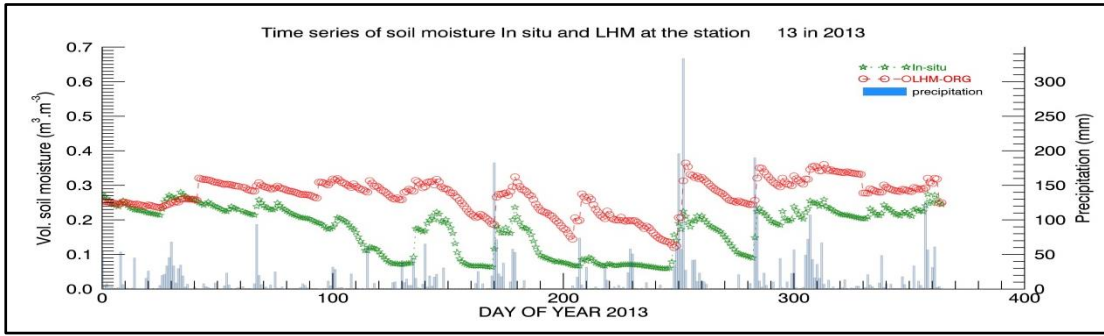
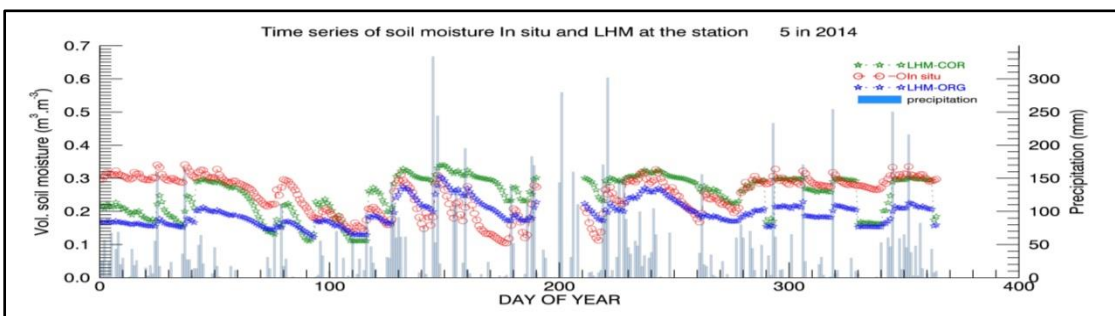
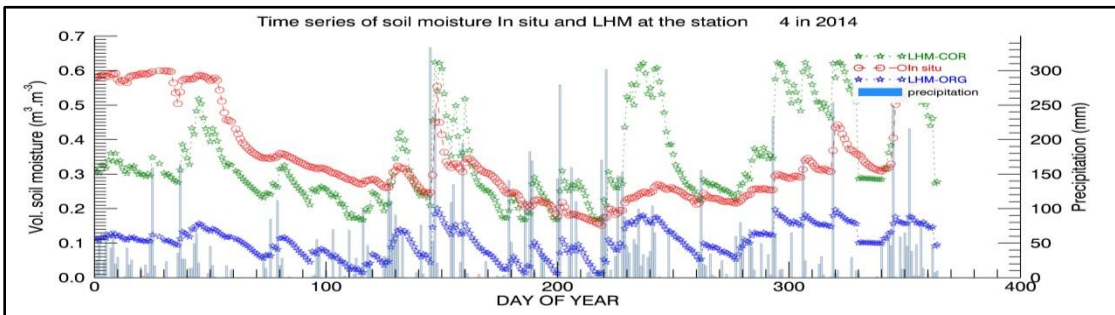
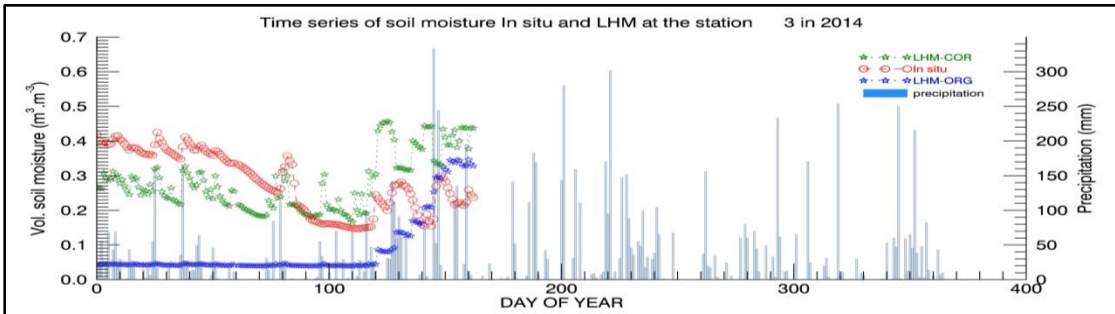
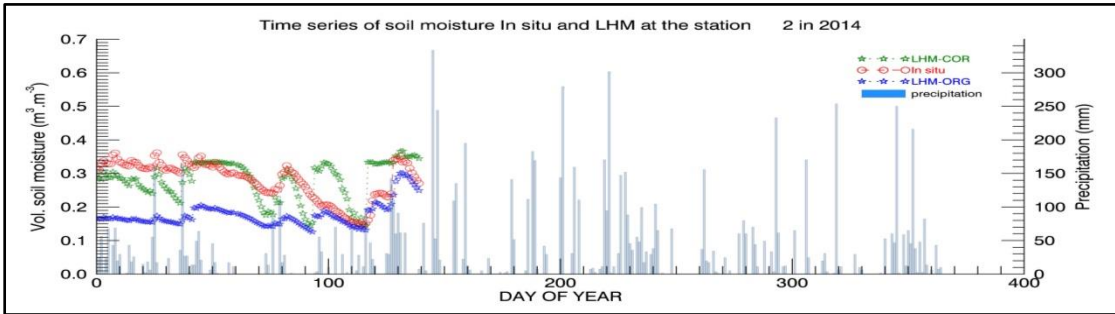
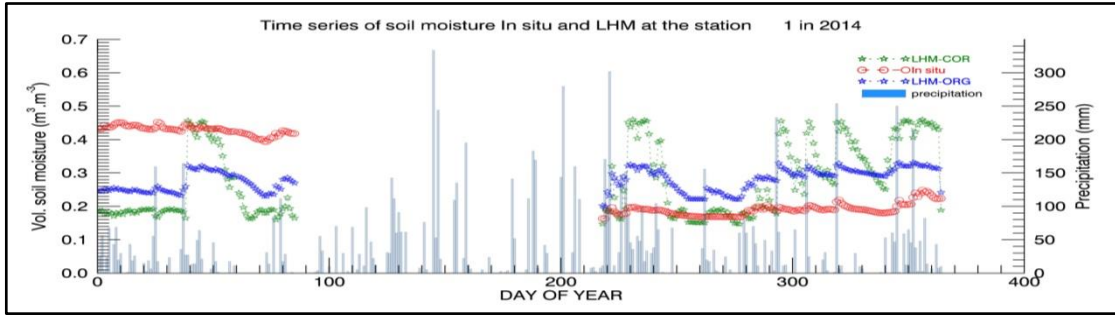
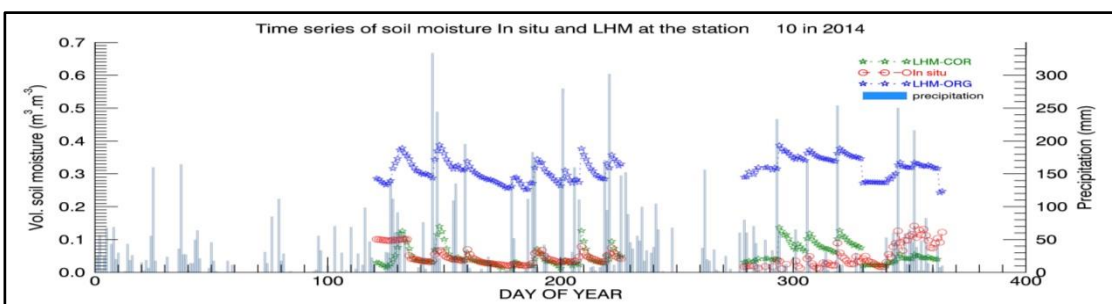
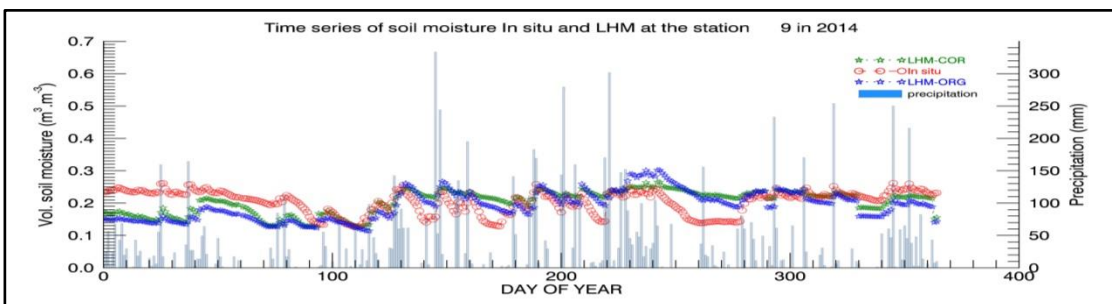
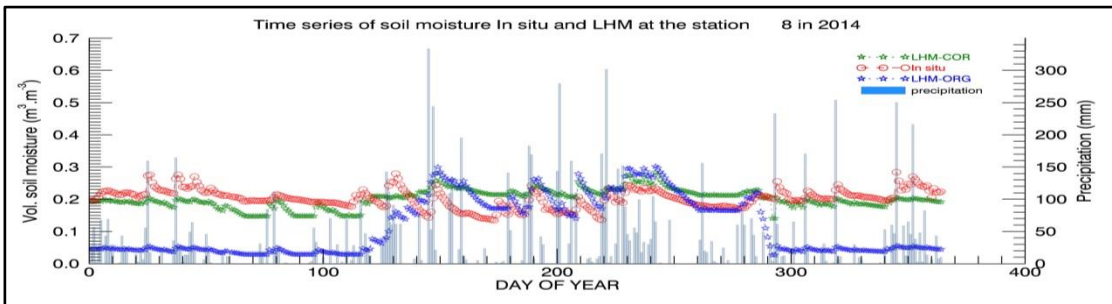
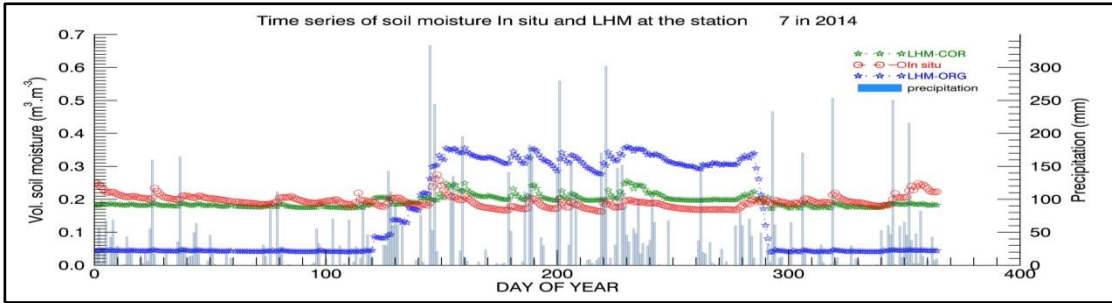
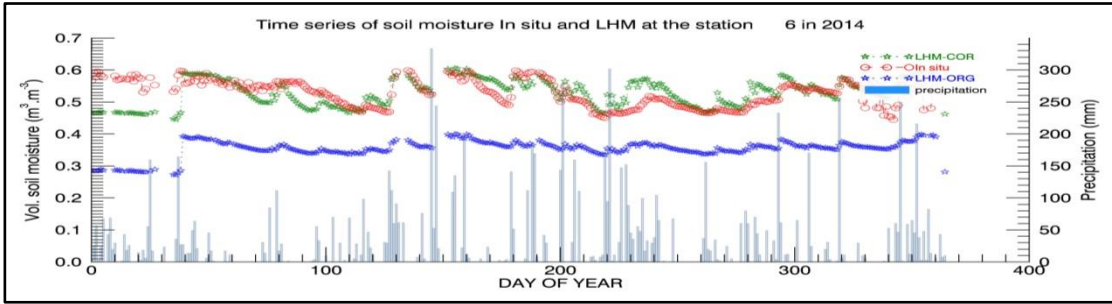
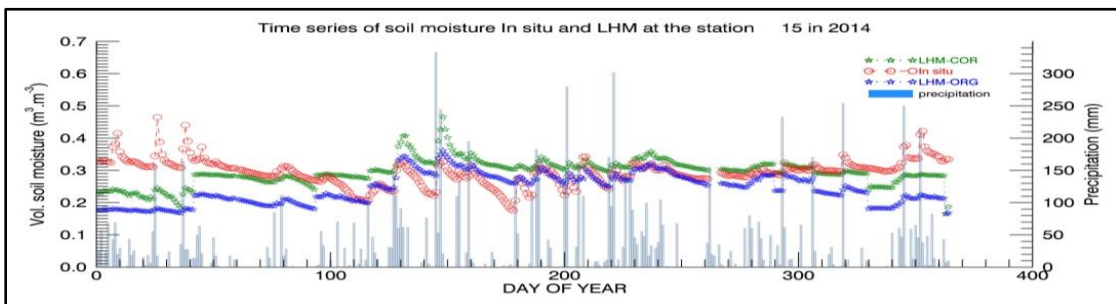
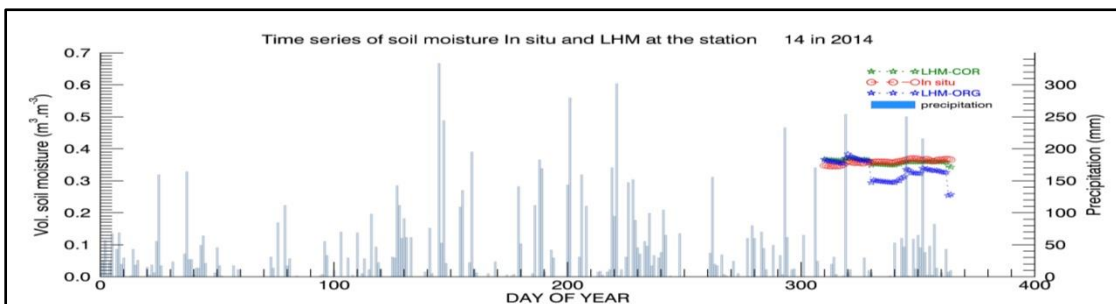
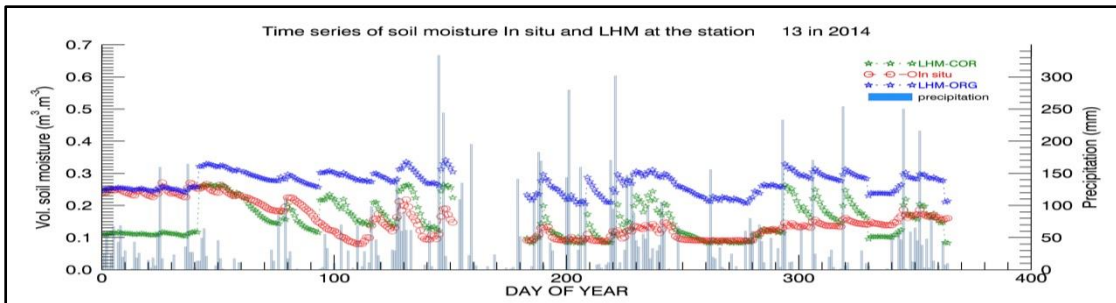
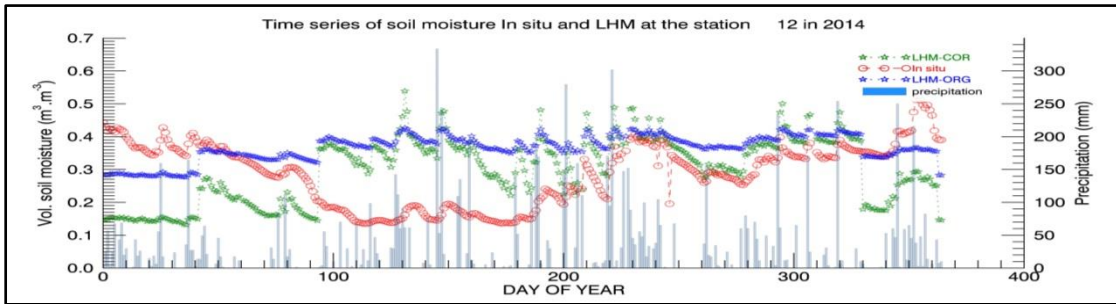
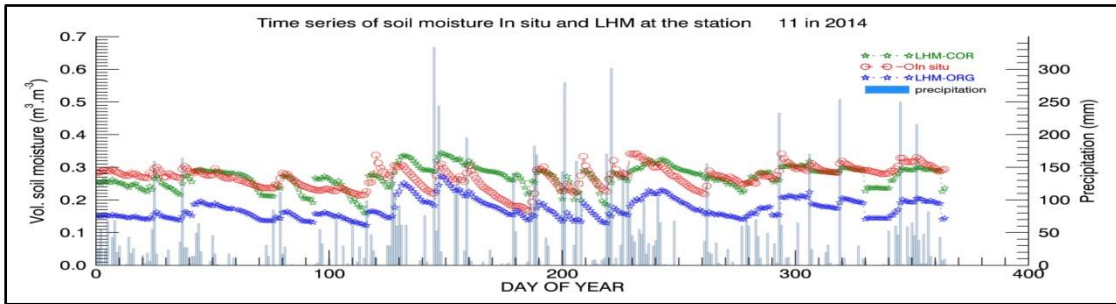


Figure 16, temporal evaluation of individual in situ measurements and simulated surface soil moisture in measurement locations along with rainfall in 2013







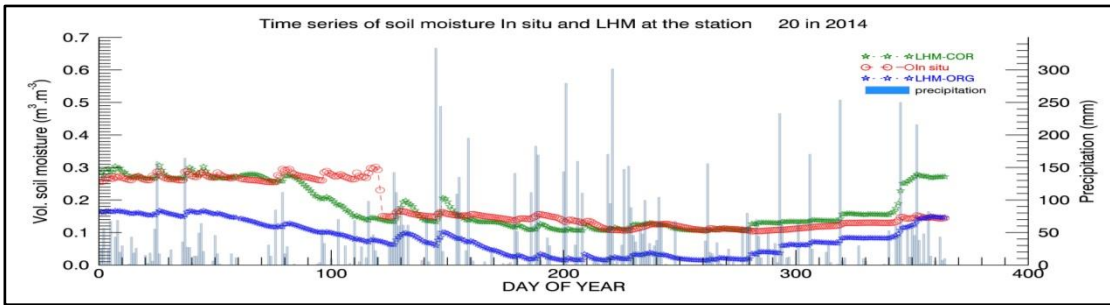
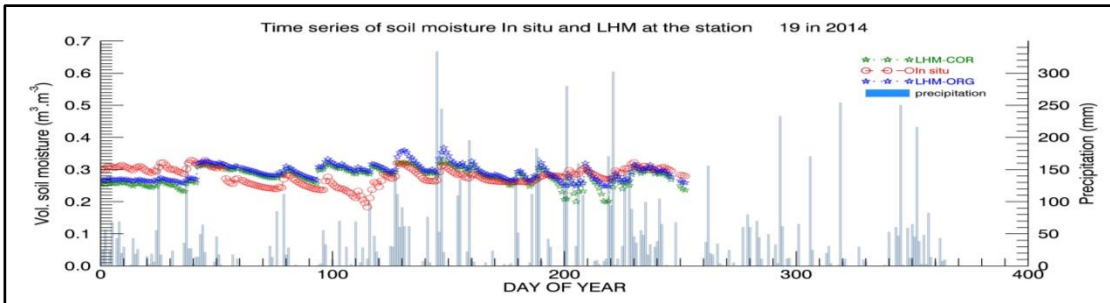
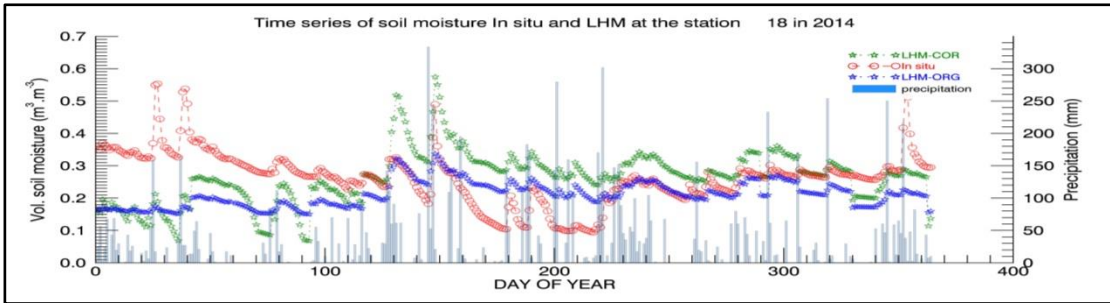
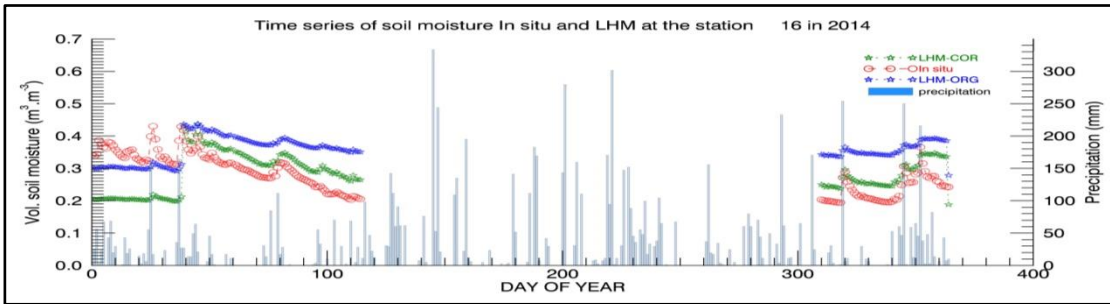


Figure 17, temporal evaluation of individual in situ measurements and simulated surface soil moisture in measurement locations along with rainfall in 2014